



# 1 A new digital Lithological Map of Italy at 1:100.000 scale for geo- 2 mechanical modelling

Francesco Bucci<sup>1</sup>, Michele Santangelo<sup>1</sup>, Lorenzo Fongo<sup>2</sup>, Massimiliano Alvioli<sup>1</sup>, Mauro Cardinali<sup>1</sup>, Laura Meelli<sup>2</sup>, Ivan Marchesini<sup>1</sup>,

<sup>1</sup> Consiglio Nazionale delle Ricerche, Istituto di Ricerca per la Protezione Idrogeologica, via Madonna Alta 126, I-06128 Perugia, Italy

<sup>2</sup> Università degli Studi di Perugia, Dipartimento di Fisica e Geologia, Piazza dell'Università 1, I-06123 Perugia, Italy  
*Correspondence to:* Michele Santangelo (michele.santangelo@irpi.cnr.it)

3

4 **Abstract.** Lithological maps contain information about the different lithotypes cropping out in an area. At variance with  
5 geological maps, portraying geologic formations, lithological maps may differ as a function of their purpose. Here, we describe  
6 the preparation of a lithological map of Italy at a scale of 1:100,000, obtained from classification of a comprehensive digital  
7 database and aimed at describing geo-mechanical properties. We first obtained the full database, containing about 300,000  
8 geo-referenced polygons, from the Italian geological survey. We grouped polygons according to a lithological classification  
9 by expert analysis of the original 5,456 unique descriptions of polygons, following compositional and geo-mechanical criteria.  
10 The procedure resulted in a lithological map with a legend including 19 classes, and it is linked to a database allowing ready  
11 interpretation of the classes in geo-mechanical properties, and amenable to further improvement. The map is mainly intended  
12 for statistical and physically based modelling of slope stability assessment, geo-morphological and geo-hydrological  
13 modelling. Other possible applications include geo-environmental studies, evaluation of river chemical composition,  
14 estimation of raw material resources.

## 15 1 Introduction

16 Lithology encodes information on the composition and physical properties of rocks and, therefore, it is a key variable in the  
17 study of earth surface and subsurface processes. As such, lithological analysis is relevant to a large body of literature, including  
18 landscape evolution (Coulthard, 2001), water flow paths (Gleeson et al., 2011), landslides (Alvioli et al., 2021; Sarro et al.,  
19 2020; Reichenbach et al., 2018), chemical composition of rivers or atmospheric CO<sub>2</sub> consumption (Donnini et al 2020;  
20 Hartmann et al., 2010; Gibbs, 1994), soil classification (de Sousa et al., 2020), soil erosion (Vanmaercke et al., 2021), seismic  
21 amplification (Mori et al., 2020; Forte et al., 2019), groundwater level variability (de Graaf et al., 2017; Lorenzo-Lacruz et al.,  
22 2017), floods (Vojtek & Vojteková, 2019), oil reservoirs (Han et al., 2018), geothermal potential (Roche et al., 2019), geo-  
23 morphological classification (Alvioli et al., 2020) and many others. Lithological variability is often a measure of geological



24 and landscape complexity, and provides important information on geological evolution and heritage (Bucci et al., 2019; Ispra  
 25 & Parco Nazionale del Cilento, Vallo di Diano e Alburni, 2013, Santangelo et al., 2013), geo-resources settings (Bucci et al.,  
 26 2016a; Ge.Mi.Na., 1962; Corpo Reale delle Miniere 1926-1935) geo-environmental risks (Giustini et al., 2019; Bentivenga et  
 27 al., 2004) and matter fluxes at the Earth's surface (Brogi & Liotta, 2011; Boni et al., 1984).  
 28 Lithological heterogeneity should be therefore sufficiently represented in maps at the local, regional and supra-regional scale.  
 29 Lithological information is commonly derived from geological maps. In recent years, much effort has been made to make the  
 30 geological data available around the world accessible at the best possible scales (Table 1, ID 1, 2). However, this still remains  
 31 an open challenge because the quality, scale, updating and availability of geodata varies enormously across the globe.

ID	Services/products/data	Type	URL	Institutions	Context
1	<i>Visualization of the Geological map of the world at the best possible scales</i>	WebMap	<a href="http://portal.onegeology.org/OnegeologyGlobal/">http://portal.onegeology.org/OnegeologyGlobal/</a>	Onegeology	Global
2	<i>General geologic map of the world at approximately 1:35,000,000 scale</i>	WebMap	<a href="https://mrdata.usgs.gov/geology/world/map-us.html#home">https://mrdata.usgs.gov/geology/world/map-us.html#home</a>	Geological Survey of Canada	Global
3	<i>Geologic Map Databases for the United States</i>	WMS, WFS, Download vector data	<a href="https://mrdata.usgs.gov/geology/state/">https://mrdata.usgs.gov/geology/state/</a>	USGS	(Sub-) Continental USA
4	<i>Pan-European and national geological datasets and services from the Geological Survey Organizations of Europe</i>	WMS, WFS, Download vector data	<a href="http://www.europe-geology.eu/onshore-geology/geological-map/">http://www.europe-geology.eu/onshore-geology/geological-map/</a>	EuroGeoSurvey	(Sub-) Continental Europe
5	<i>Geoportal of the Italian Geological Survey (ISPRA)</i>	WMS, WFS, Download vector data	<a href="http://sgi2.isprambiente.it/viewers/gi2/">http://sgi2.isprambiente.it/viewers/gi2/</a>	ISPRA	National Italy
6	<i>Visualization of the available (in raster format) geological sheets of Italy at 1:100.000 scale</i>	Web application	<a href="http://sgi.isprambiente.it/geologia100k/">http://sgi.isprambiente.it/geologia100k/</a>	ISPRA	National Italy
7	<i>Visualization of the available (in raster format) geological sheets of Italy at 1:50.000 scale</i>	Web application	<a href="https://www.isprambiente.gov.it/Media/carg/index.html">https://www.isprambiente.gov.it/Media/carg/index.html</a>	ISPRA	National Italy
8	<i>Guidelines for the realization of the Geological and Geotechnical Map at the scale 1:50.000</i>	Web Page	<a href="https://www.isprambiente.gov.it/en/projects/soil-and-territory/carg-project-geologic-and-geothematic-cartography">https://www.isprambiente.gov.it/en/projects/soil-and-territory/carg-project-geologic-and-geothematic-cartography</a>	ISPRA	National Italy
9	<i>REST service provided by ISPRA for the publication of spatial data</i>	REST	<a href="http://sgi2.isprambiente.it/arcgis/rest/services/servizi/carta_geologica_100k/MapServer/">http://sgi2.isprambiente.it/arcgis/rest/services/servizi/carta_geologica_100k/MapServer/</a>	ISPRA	National Italy

33 **Table 1:** Uniform Resource Locators (URL) of the institutional services, guidelines, products or datasets consulted for compiling our map.  
 34 Links were last accessed on 14 January 2022.

35  
 36 The situation is more homogeneous at the continental or sub-continental level. For example, in 2017 the U.S. Geological  
 37 Survey published a compilation of the individual releases of the Preliminary Integrated Geologic Map Databases (SGMC) for  
 38 the United States (Table 1, ID 3), which represents a seamless, spatial database of 48 State geologic maps that range from  
 39 1:50,000 to 1:1,000,000 scale (Horton, 2017). The SGMC is not a truly integrated geologic map database because geologic  
 40 units have not been reconciled across State boundaries. However, the geologic data contained in maps for individual States  
 41 have been standardized to allow spatial analyses of lithology, age, and stratigraphy.



42 In Europe, in 2016 the EuroGeoSurvey launched the European Geological Data Infrastructure (EGDI, Table 1, ID 4). EGDI  
43 provides access to Pan-European and national geological datasets and services from the Geological Survey Organizations of  
44 Europe. Geological Layers available include the Geological map of Europe, 1:5,000,000 scale, and the surface lithology of  
45 Europe, 1:1,000,000 scale. More detailed geologic or geological derived maps only are available at national scale (Table 1, ID  
46 5, 6).

47 In Italy, the existing geological maps with national coverage (Console et al., 2017) are at 1:1,250,000 (Bonomo et al., 2005)  
48 1:1,000,000 (Pantoloni, 2011; Cipolloni et al., 2009; Compagnoni, 2004), 1:500,000 (Compagnoni et al., 1976-1983), and  
49 1:100,000 scale (Servizio Geologico d'Italia, 2004) and are managed by ISPRA (Istituto Superiore per la Protezione e la  
50 Ricerca Ambientale - De Logu et al., 2012). The 1: 50,000 national geological map, coordinated and published by ISPRA, has  
51 an incomplete coverage of the entire Italian territory (Table 1, ID 7, 8).

52 Some of the maps mentioned above are accessible, for display purposes only, via standard view services (WMS -Web Map  
53 Service, Table 1, ID 5).

54 Amanti et al., (2007) and (2008), described the first known attempt by ISPRA to draft a lithological map of Italy at the  
55 1:100,000 scale. The published map covers the 65% of the national territory and does not include Sardinia, Sicily and the  
56 sheets 156 to 176, 183 to 187 and 196 to 199. This lithological map is not accessible in raster or vector format.

57 In 2018, ISPRA completed the work published in the 2007 and 2008 publications, and a lithological cartography of the entire  
58 Italian territory at 1:100,000 scale, was made accessible for visualization, through the geo-portal (Table 1, ID 5). The map  
59 was obtained gathering information from the 277 sheets of the Carta Geologica d'Italia, adopting a unique legend model to  
60 produce a homogeneous lithological map of the whole country.

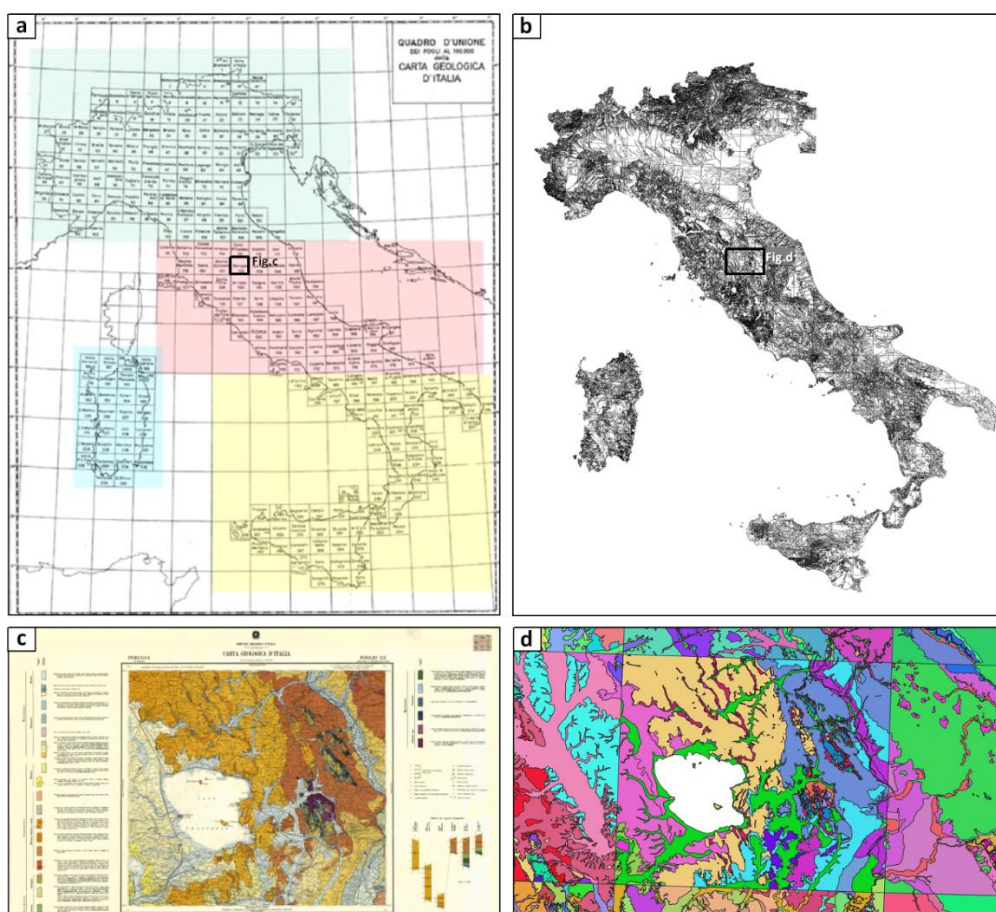
61 However, specific applications in different geosciences fields require distinct criteria and methods to elaborate different  
62 lithological classifications. For example, starting from the geological maps produced by ISPRA at the 1:100,000 scale, a geo-  
63 lithological map of Italy was recently classified according to the expected seismic behaviour of the material (Forte et al. 2019),  
64 although the map is only represented as a figure along the paper, and not available for download or visualization.

65 Here, we describe a new lithological map of Italy (LMI), entirely available for download, aimed at differentiating lithotypes  
66 based on their expected geo-mechanical properties in relation to slope stability and with the specific purpose of being used in  
67 statistically based (Reichenbach et al., 2018; Schlogel et al., 2018; Alvioli et al., 2016; Rossi et al., 2016) and physically based  
68 (Alvioli et al., 2021, 2016; Mergili et al., 2014; Raia et al., 2013) slope stability models. Early versions of the map described  
69 in this work were used for geo-morphological analysis and terrain classification (Alvioli et al., 2020) and for rockfall  
70 susceptibility assessment (Alvioli et al., 2021). The map and the associated database were designed in a versatile way. They  
71 can be easily enhanced/reclassified using different or additional criteria, e.g., considering age, tectonic or geotechnical  
72 information, and thus can be relevant to a wide range of studies.



## 73 2 Data

74 LMI was prepared starting from the data of the 277 sheets of the geological map of Italy at 1:100,000 scale (Table 1, ID 6),  
75 provided by the Italian Institute for Environmental Protection and Research (ISPRA – Italian geological survey; *Servizio*  
76 *Geologico d'Italia*, 2004) available as a digital database through the ISPRA website. The website exhibits a representational  
77 state transfer (REST) service for the publication of spatial data (Table 1, ID 9), and distributes the geological map of Italy at a  
78 scale of 1:100,000, in vector format (Figure 1). The map contains 294,266 topologically correct polygons, and 5,477 unique  
79 descriptions of the geological formations. The scanned versions of the original geological sheets are also available for  
80 consultation (Table 1, ID 6).



81  
82 **Figure 1:** (a) The 277 sheets of the geological map of Italy at 1: 100,000 scale as visualized at the ISPRA website (URL in Table 1, ID 6).  
83 The location of figure (c) is indicated; (b) All the unclassified 292,705 vector polygons available in the source dataset. The location of figure  
84 (d) is indicated; (c) Published version of the sheet n. 122 “Perugia” (Servizio Geologico d’Italia, 1968a) as visualized in raster form at the  
85 ISPRA website (URL in Table 1, ID 6); (d) Randomly coloured polygons within the area encompassing the sheet n. 122. Polygons having  
86 the same geological description in the original attribute table (field: NAME) provided by ISPRA (URL in Table 1, ID 9) assume the same



87 colour. The area also encompasses the straight boundaries with its surrounding four geological sheets, clearly visible as sharp colour changes  
 88 along NS and WE oriented straight lines.

89

90

91 The attribute table associated with the polygons originally contained a unique numeric identifier and the description of the  
 92 geological unit as specified in the original geological maps (field: *NAME*). Comparison between the original legend  
 93 descriptions and the text reported in the description field revealed that several simplifications were made. Such differences  
 94 represented a major source of inhomogeneity within the database, which limited the efficacy of using automated database  
 95 queries to apply the new lithological classification scheme. Table 2 reports examples of such simplifications of the original  
 96 legend.

97

Simplifications and Problems in the Name_Ulf column	NAME Descriptions	Geological Sheet numbers	Approach to the issues	Original Descriptions
<i>Lack of information concerning the name of the formation, the lithology and the internal architecture</i>	undifferentiated	92-93	SQ+ancillary	Sericitic, quartz-sericitic, chloritic schists, of Permian age, prevalent, not separable cartographically from schistose limestones because of the minute mixture determined tectonically
<i>Lack of information concerning the name of the formation and the lithology</i>	lenticular alternations	130	SQ+ancillary	Lenticular alternations, of variable extension and power, consisting of: clay and varicolored marl, calcarenite, calcareous breccia, sandstone, limestone and marly limestone.
<i>Lack of information concerning the lithology</i>	Corleto Perticara formation	200	SQ+ancillary	Violet, brown and yellowish clayeyes, gray and white clayey marls, subordinately red, calcareous marls and marly limestones of gray or greenish color, gray calcarenite or gray quartzarenites with siliceous cement.
<i>Only partial lithological information</i>	Corleto Perticara formation - marne	199	SQ+ancillary	Clayey marl gray and subordinately red; calcareous marl and marly limestone of gray or greenish color, calcarenite and sandstone.
<i>Identification of a rock unit with local/informal denomination</i>	“metallifero bergamasco”,  “biancone”	7-18  35, 36, 49, 22,38	SQ+ancillary	Well stratified black limestones, often with parallel lamination and pisolithic at the base; dolomite intercalations in the lower part.  White compact limestones; greyish or gray limestone; black marly, bituminous limestone; greenish marl; ceroid limestones with chert.
<i>Formations made up of several members</i>	sandstones, quartzites, phyllites, schistose sandstones, argilloscist	226	SQ+ancillary	Sandstones, quartzites, phyllites, schist sandstones, more or less philladic clayey, alternating, sometimes even minute.
<i>Typos</i>	“scisti di ?dolo”	7-18	Q	“Scisti di Edolo”
<i>Singular/plural</i>	moraine/moraines	30, 31, 32, 17, 20, 12, 132, 140, 145, 151, 152, 160, 209, 210 /151	Q	Moraine/Moraines
<i>Uppercase/lowercase</i>	Moraine/moraine	62/25, 24, 22, 4 <sup>b</sup> , 22, 6, 8, 18, 19, 33, 34,	Q	Moraine



		5, 15, 16, 27, 28, 29, 41, 55, 66		
<i>Mangled names in some sheets</i>	“majolica” in place of “maiolica”	139	Q	“Majolica”
<i>Spelling errors</i>	“ammessi subvulcanici”	11	Q	“Ammassi subvulcanici”
<i>Use of accents</i>	“unità di sillano”	108	Q	“Unità di Sillano”
<i>Use of apostrophes</i>	“marne e calcari dell'antola”	84, 85	Q	“Marne e calcari dell'Antola”
<i>Use of percentage</i>	soils containing more than 10% of organic substances	76	Q	Soils containing more than 10% of organic substances
<i>Use of special character letters</i>	würmian moraines	54, 42, 67, 4, 1-4 <sup>a</sup> , 14, 14 <sup>a</sup> , 91	Q	Würmian Moraines

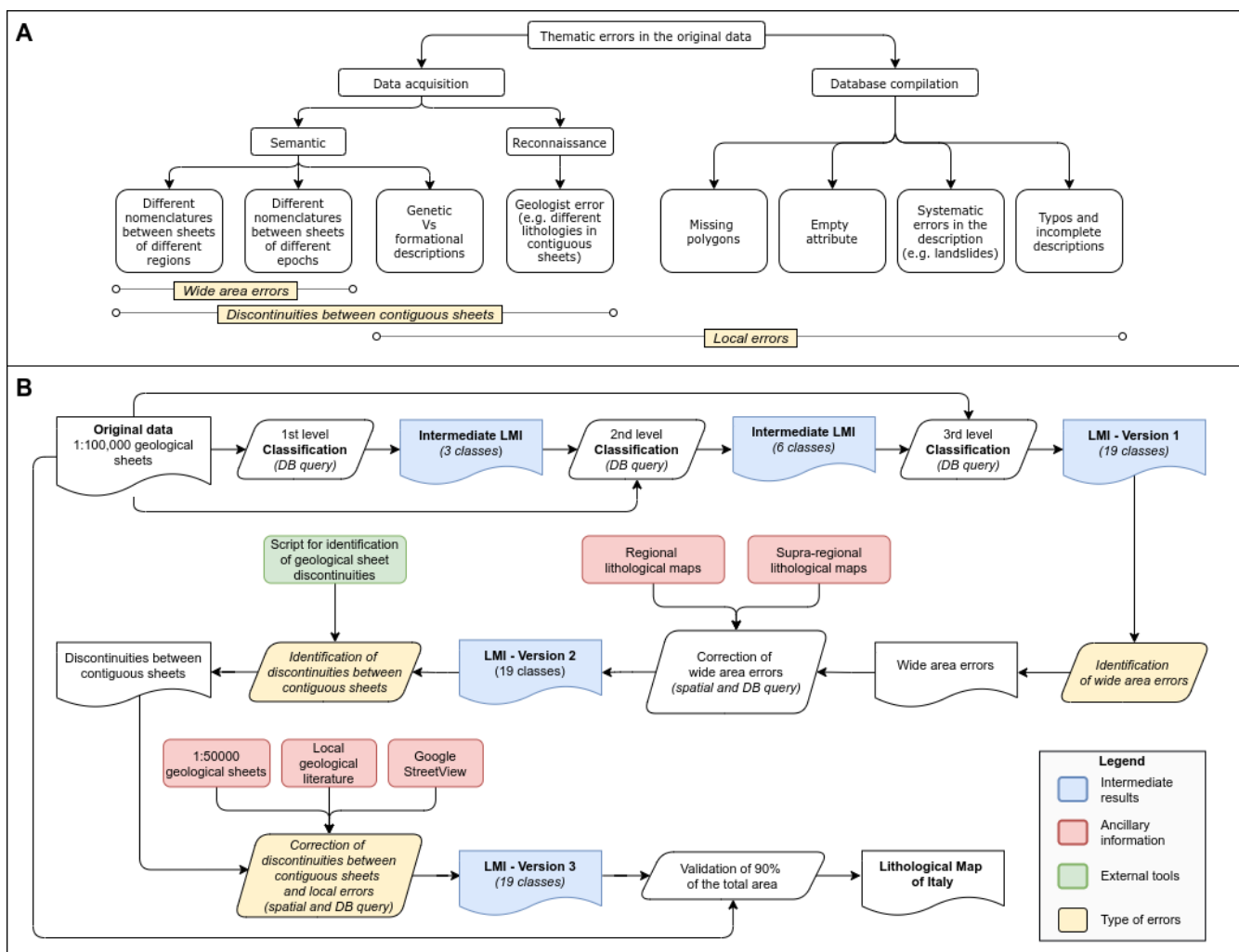
**Table 2:** Examples of simplifications and problems related to the unique rocks descriptions contained in the source dataset, and comparison with the original description in the legend of the original geological sheets. Depending on their nature, issues were approached using database queries (Q), spatial queries (SQ), and ancillary material (regional/local geological maps and literatures).

In most cases, the text corresponds only to the first word or lemma of the original description. In the case of formations made up of several members, the *NAME* field contains a lemma indicating the main lithological members, but this approach is not consistent for all records. In some cases, the polygons correspond to empty records in the attribute table (most of them refer to lakes or inland waters); in others, the polygons are absent and were added in this work to fill in empty areas, according to the information checked in the original geological sheets. Overall, the analysis of the database revealed several types of errors affecting the source data set, which are summarized in Figure 2a. We refer to errors in the database as *thematic errors*, since the attribute assigned to a polygon is incorrect or not corresponding to the ground truth (assumed here to be the original geological sheets). Thematic errors in the database can be grouped according to two main categories: *inconsistency between surveyors*, and *errors of the operators* who compiled the database. We call the first “*Data acquisition errors*” and the second “*Database compilation errors*”.

*Data acquisition errors* are related to individual mapping errors (*Reconnaissance errors*, in Figure 2a) or to disused, or dialectal/jargon geological descriptions (*Semantic errors*, in Figure 2a). Figures 3a and 3c show typical errors related to subjectivity issues visible at the boundary between geological sheets drafted by different working groups and published many years apart from each other (Console et al. 2017). Figure 3c also contains references to local or dialectal terms that may escape general lithological classification criteria. Subjectivity errors related to disused, inadequate or dialectal geological description and terms were systematically resolved (Figure 3d) by using database queries. Despite our effort, little to nothing could be done for most of the errors due to contrasting classification of rock assemblages by individual geologists or the working groups who compiled the original geological sheets. Such problems still remain in our lithological map (Figures 3b,d). A new national



120 geological survey currently in progress (Carg project, Table 1, ID 7, 8) will likely resolve criticalities of geological  
 121 interpretation, which is beyond the scope of this work.

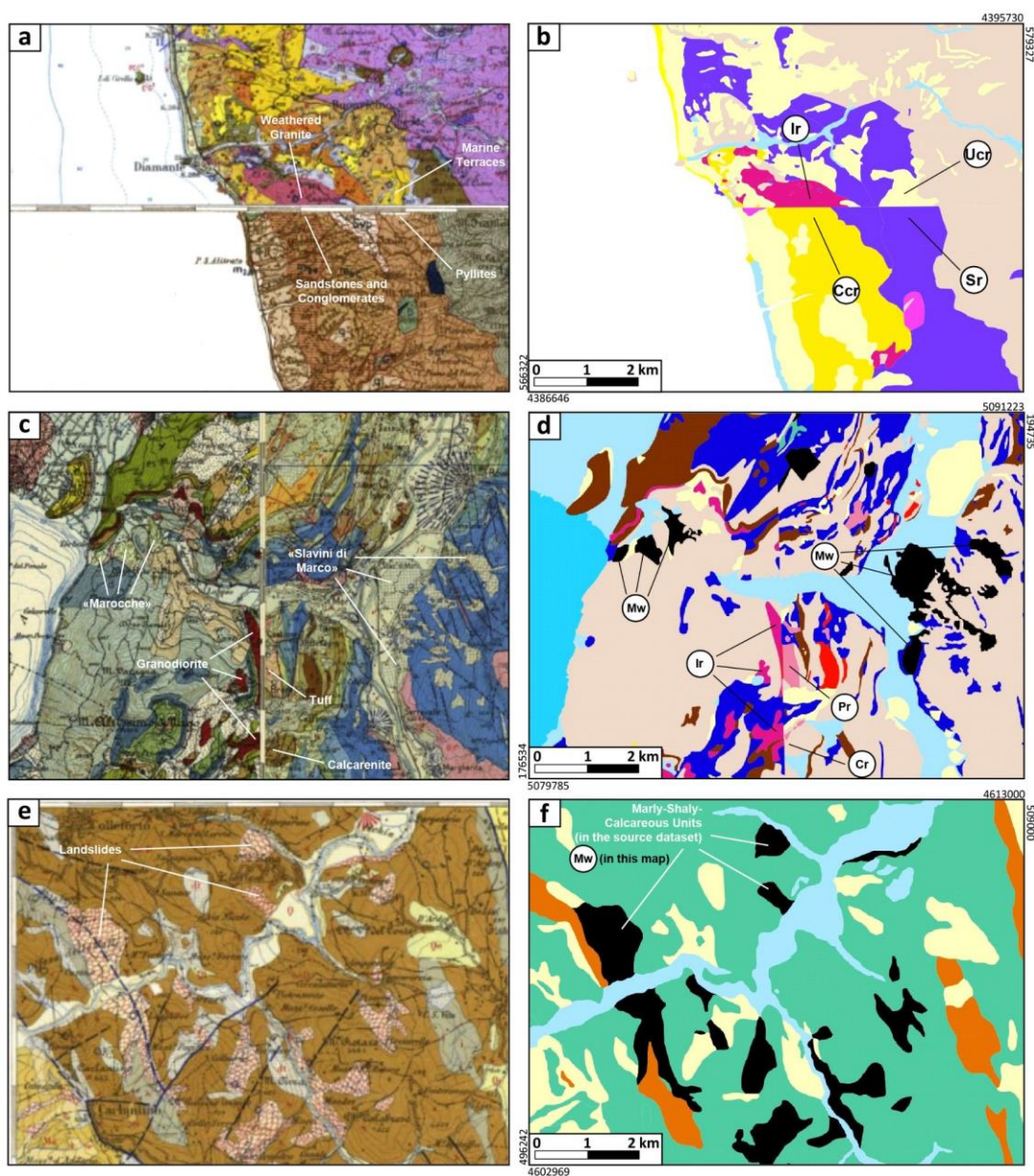


122  
 123 **Figure 2:** (a) Scheme of the main thematic errors identified in the source dataset. Errors can be related to (i) uncorrected or incomplete  
 124 database compilation or (ii) to data acquisition as a consequence of individual errors or inhomogeneity in the use of geological nomenclature,  
 125 description and interpretation; (b) Flowchart of the classification process of the Lithological Map of Italy

126  
 127 *Database compilation errors* can be systematic (Figure 3f) and occasional. Figure 3f refers to a systematic thematic error  
 128 dealing with the compilation of the *NAME* column of some landslide polygons with the description of a lithostratigraphic unit  
 129 clearly unrelated to landslides. As exemplified in Figure 3f, the compilation errors were identified and corrected during the  
 130 reclassification of the source dataset.



131



132

133 **Figure 3:** Main problems of the source dataset highlighted through the comparison of representative areas, as appear respectively in the  
 134 published raster version of the geological sheets (a, c, e) and in the our reclassified vector map (LMI) (b, d, f) - Vector Map Legend - Ir  
 135 (Intrusive rocks), Ucr (Unconsolidated clastic rocks), Ccr (Consolidated clastic rocks), Sr (Schistose rocks), Pr (Pyroclastic rocks), Cr  
 136 (Carbonatic rocks), Mw (Mass wasting); Example of errors related to locally wrong rocks classification and inhomogeneity problems at the  
 137 boundary between geological sheets of different years are shown in (a) (year 1969 - N sheet n. 220 vs year 1900 - S sheet n. 228) and in (c)  
 138 (year 1948 - W sheet n. 35 vs year 1968 - E sheet n. 36); Examples of local/dialectal terms in the geological description are shown in (c)  
 139 (“Marocche” and “Slavini di Marco” for Mass wasting); Examples of errors related to incorrect database compilation are shown comparing



140 (e) and (f). Figures **a, c, e**, include sheets number **220, 228, 35, 36, 163** as visualized in raster form at the ISPRA website (URL in Table 1,  
141 ID 6). Sources: (a) upper image is from Servizio Geologico d'Italia (1970c), lower image from R. Ufficio Geologico (1900). (c) Left image  
142 from Ministero dei lavori pubblici ufficio idrografico sezione geologica (1948), right image from Servizio Geologico d'Italia (1968b). (e)  
143 Image from Servizio Geologico d'Italia (1964).

### 144 **3 Methods**

145 The procedure adopted to carry out the new Lithological map of Italy (LMI) is described in Figure 2b. Starting from the original  
146 data (top left in Figure 2b) we derived the LMI (bottom right in Figure 2b) through the following steps: (a) definition of a  
147 procedure including alphanumeric queries, geospatial analysis and expert judgements; (b) preparation of at least two  
148 intermediate products and three versions of the LMI.

149 The “*Intermediate LIM - 3 classes*” product (Figure 2b) follows a genetic criterion and describes (i) magmatic, (ii)  
150 metamorphic and (iii) sedimentary rocks.

151 The “*Intermediate LIM - 6 classes*” product (Figure 2b), distinguishes (i) older (typically Pre-Neogene in age) and structured  
152 substratum-derived sedimentary rocks and (ii) magmatic intrusion, from (iii) younger (Neogene and Quaternary in age) less to  
153 not deformed sedimentary and magmatic covers rocks. Sedimentary cover was further separated in (iv) undifferentiated and  
154 (v) alluvial/marine rocks, while the (vi) metamorphic rocks class remains unchanged.

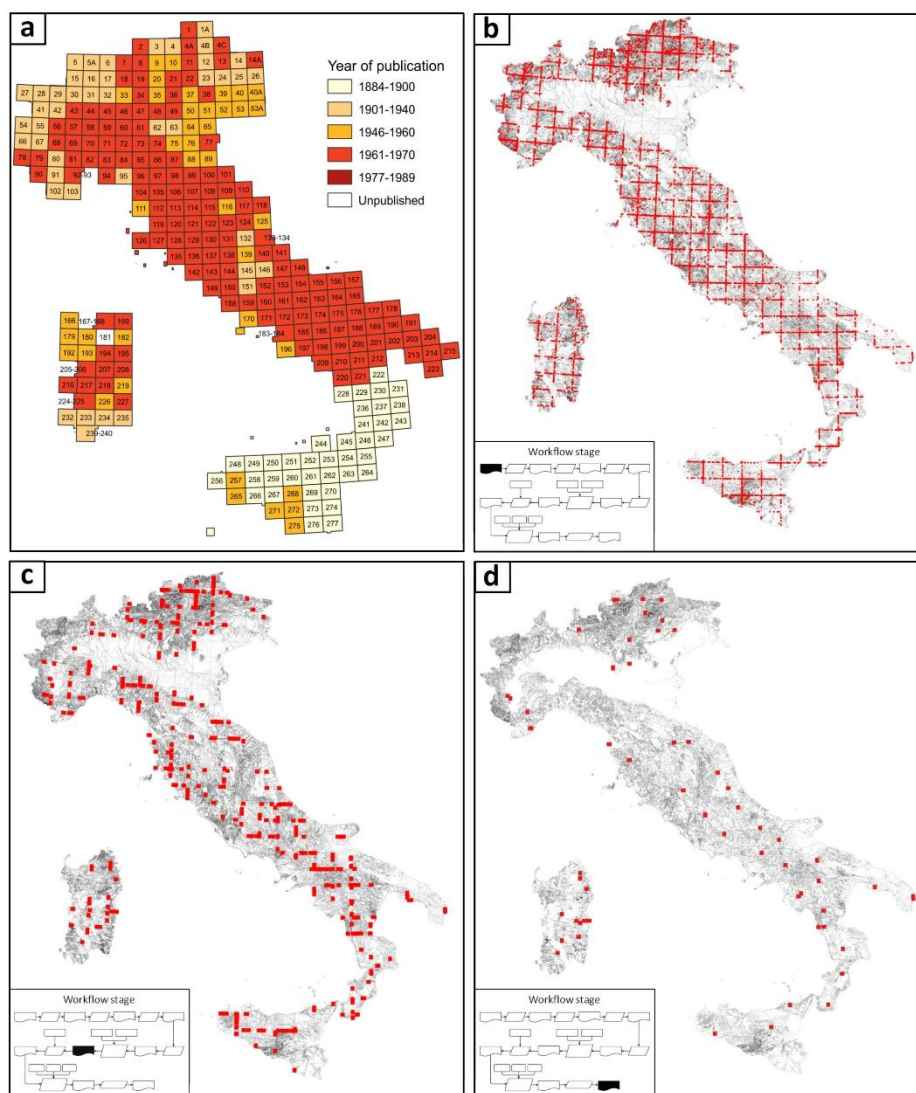
155 “*LMI - Version 1*” (Figure 2b) is based on a predominantly lithological criterion, and contains the 19 classes defined in our  
156 legend.

157 To translate different rock type information into lithological classes, the dominant rock types were emphasized assuming that  
158 rocks mentioned foremost are more abundant than those mentioned later in the descriptions. This classification strategy is  
159 consistent with many mapping guidelines (UNESCO-IUGS, 2016; Hartmann et al., 2012; Asch, 2005), and it is based on the  
160 classification system by Dürr et al. (2005), with modifications. Determining the dominant rock types within a unit was not  
161 always straightforward, though. Cases of uncertainty about the dominant rock type were found and were resolved by  
162 considering specific lithological classes defined by the combination of the most representative rock types. For example, the  
163 rock unit named “Clays and Limestones”, composed in equal parts of both lithotypes, was assigned to the class “mixed  
164 sedimentary rocks”, which also contains other sediments where carbonates are mentioned but not dominant.

165 Each classification step (“1st, 2nd, 3rd level” in Figure 2b) used the result of the former step (where applicable) and the original  
166 data to build complex alphanumeric database queries. No spatial queries were involved. Furthermore, the first two (coarser)  
167 levels of classification (intermediate products) helped underlining systematic semantic and compilation errors throughout the  
168 database. For example, rock units containing the word “schist” were consistently classified as “metamorphic rocks” in the first  
169 level classification, which led to classifying sedimentary rocks with a strong pelitic component as metamorphic rocks. This  
170 happened since such sedimentary rocks were commonly improperly indicated as “schists” in geological descriptions dating



171 over 50 years. Similarly, the words “clays” and “claystones”, or “sands” and “sandstones”, were sometimes used as synonyms  
172 in the original geological legend, with consequent uncertainty between the sedimentary cover or the sedimentary substratum.  
173 Inconsistencies of the source data set mainly derive from the large variability of the level of detail of the original geologic  
174 descriptions between different geological sheets. Compilation of the 277 geological sheets of the entire National territory  
175 required 92 years, from 1884 to 1976 (Figure 4a), which inevitably led to differences in the geological descriptions (and  
176 interpretation) between old and recent sheets.  
177



178



179 **Figure 4:** (a) The 277 sheets of the geological map of Italy at 1: 100,000 scale classified according to the years of publication, modified  
180 after Console et al. (2017); (b) The 12711, NS-EW oriented segments (red lines) having different lithotypes in the two sides and sinuosity  
181 equal to 1. (c) The 405 Red lines longer than 1000 m left after semi-automatic classification. The unclassified 294,266 vector polygons of  
182 the source dataset are shown as background in (b) and (c); (d) the 58 Red lines longer than 1000 m left after the expert analysis of the semi-  
183 automatic output. The unclassified 100,705 vector polygons derived from the dissolve GIS operation performed after the classification phase  
184 are shown as background. Insets in (a), (b), and (c) indicate the classification stage to which each map refers, according to the scheme in  
185 figure 2b.  
186

187 A similar issue was introduced between sheets or regions mapped by different authors and working groups (Figures 3a,c). As  
188 a consequence, problems of inhomogeneity were found in the descriptions of litho-stratigraphic units, which in turn generated  
189 problems of harmonization at the boundary between different geological sheets. To mitigate inhomogeneity problems, we  
190 decided to adopt broad categories in the classification of the third level as a function of similar lithology, genetic processes  
191 and expected geotechnical behaviour. With this aim, rock descriptions were generalized into 19 lithological classes. However,  
192 harmonizing the original 5,477 univocal descriptions of the geological units in 19 simplified lithological classes was often  
193 tricky and required expert judgement supported by the consultation of regional and supra-regional geo-lithological maps (Conti  
194 et al., 2020; Piana et al., 2017; Lentini & Carbone, 2014; Carmignani et al., 2013; Vezzani et al., 2010; Celico et al., 2005;  
195 Carmignani, 2001; Consiglio Nazionale delle Ricerche, 1990; Amodio Morelli et al., 1976). We used a very long and complex  
196 set of database queries to classify and harmonize the data. For example, to correctly classify glacial drift avoiding possible  
197 overlapping with alluvial deposits, we requested the NAME field to either contain strings with the words "wurm", "würm",  
198 "glacial", "moraine", and at the same time without any of the words "alluvial", "fluvial" and "terrace". Due to their specificity,  
199 queries were generally longer and more complex when used to classify widespread lithological classes containing a large  
200 number of unique descriptions. The *LMI - Version 2* is the product of this harmonization phase where "wide area errors" were  
201 corrected (Figure 2b), resulting in a lower number of discontinuities at the boundaries of regions or individual geological  
202 sheets, compared to these contained in the *LMI - Version 1* (Figure 4 b,c).

203 To identify discontinuities between contiguous geological sheets (Figure 2b) we developed an automatic procedure based on  
204 the analysis of the lithological classes located to the right and left of each lithological boundary. We selected all EW and NS  
205 oriented straight boundaries longer than 1 km and resolved classification inconsistencies across such boundaries by expert  
206 judgement. Discontinuities between contiguous geological sheets are due to inconsistencies between surveyors. Since we  
207 assumed that the ground truth is the original geological sheets, our approach consisted in assuming only one of the two  
208 contiguous polygons was to be corrected. If available ancillary data allowed to confirm one of the two bounding polygons  
209 attribute, classification of the second polygon was amended accordingly. Otherwise the discontinuity was solved by assigning  
210 the class that minimised discontinuities and inconsistencies.

211 To reduce the number of discontinuities between contiguous sheets, we consulted geologic maps available at scale 1:100,000  
212 (Servizio Geologico d'Italia, 1970a,b,c,d,e, 1969, 1968a,b, 1965, 1964, 1955; Ministero dei Lavori Pubblici, Ufficio  
213 Idrografico, Sezione Geologica, 1948; R. Ufficio Geologico, 1884a,b,c,d,e, 1900) and at a scale of 1:50,000 (Servizio



214 Geologico d'Italia, 2016, 2015a,b,c, 2014, 2012a,b,c, 2011a,b,c,d, 2010a,b,c, 2009a,b, 2008, 2006, 2005a,b,c,d, 2002, 1973,  
215 1972), where available. Where information on rock types was unavailable from the national maps, we obtained the descriptions  
216 of the named stratigraphic units from regional and local geological maps and from the scientific literature (Novellino et al.,  
217 2021; Bucci et al., 2020, 2016, 2014, 2012; Vignaroli et al., 2019; Mirabella et al., 2018; Ronchi et al., 2011; D'Ambrogi et  
218 al., 2010; Brozzetti, 2007; Chiarini et al., 2008; Giannandrea et al., 2006; Schiattarella et al., 2005; De Rita et al., 2004; Girotti  
219 & Mancini, 2003; Catanzariti et al., 2002; Bortolotti et al., 2001; Prosser, 2000; Giardino & Fioraso 1998; Tavarnelli, 1997;  
220 Campobasso et al., 1994; Centamore et al., 1991; Patacca et al., 1991). The quality of the literature was variable, and may have  
221 introduced some uncertainty. In some rare locations, the rock type information of digital geological map vector datasets was  
222 derived from paper maps, which were georeferenced and visually assigned to the units of the digital maps. In specific and rare  
223 cases, it was necessary to use Google Earth and Google Street View to study and display images of outcrops for a local visual  
224 analysis. After this finer phase of correction, a total of 58 segments longer than 1000 m remained unsolved since they would  
225 require the geometry of the original polygons to be modified (Figure 4d). The problem greatly increases for the classification  
226 inconsistencies along segments shorter than 1,000 meters, for which a systematic correction was out of the scope of this work.  
227 After the classification phase, boundaries were dissolved to merge adjacent polygons sharing the same lithology. With this  
228 streamlining operation, the number of polygons has dropped from 294,266 to 180,503. The result of the correction of  
229 discontinuities between contiguous sheets is the *LMI - Version 3* (Figure 2b).

230 Eventually, we performed a validation of the map *LMI - Version 3* (Figure 2b). First, the area percentages of all the unique  
231 descriptions within each class were computed and sorted in descending order. Then, within each lithological class, all the  
232 unique descriptions summing to a total area of 90% of that class were inspected for possible inconsistencies, by comparing  
233 and verifying the assigned lithology with the original description in the field NAME. The total area validated corresponds to  
234 271,651.56 km<sup>2</sup>, which represents ~90% of the Italian territory and includes 1,702 different geological descriptions. For each  
235 lithological class, polygons of a very small size, between 0.05% and 0.8% of the area of the lithological class itself, were  
236 validated (Table 3). The remaining 10% of the total area of each lithological class, which consists of 4,632 records associated  
237 with negligible percentage values of the area (on average 0,06% of the total area of each class), was not checked. It is worth  
238 noting (Table 3) that the Carbonate rocks class (Cr) accounts for most of the descriptions (1,155), followed by Unconsolidated  
239 clastic rocks (Ucr), Alluvial and marine deposits (Al) and Siliciclastic sedimentary rocks (Ssr) which include 856, 583 and 560  
240 descriptions respectively. However, the areal extent of these four classes (the most represented on the territory) does not reflect  
241 the number of descriptions, as the most extensive class is Al (75,424.36 km<sup>2</sup>), followed by Ucr (45,764.12 km<sup>2</sup>) and then Cr  
242 and Ssr (45,329.81 km<sup>2</sup> and 34,099.68 km<sup>2</sup>, respectively).

243 We checked all of the records classified as anthropogenic deposits (12 records), landslides (26 records), lakes and glaciers (10  
244 records) (Table 3). Some errors inherited from compilation errors of the source dataset, also emerge from the validation as  
245 classification inconsistencies. To give an example of this kind of errors we report a case from the landslide class, in which the



246 most representative (21% of the area, with respect to the total landslide class) unique descriptions are defined as “clayey and  
 247 calcareous turbidites of Paleogene age”. These same polygons were, instead, correctly represented as landslides in the original  
 248 geological sheet in raster format (Figure 3e). Wherever possible, polygons classified as landslides were manually corrected by  
 249 looking at the original raster map. Similar errors concerning other geological descriptions were treated using the same  
 250 approach. After validation, the final *Lithological Map of Italy* (LMI) was produced (Figure 2b).

Lithologic class	N. object (#)	A. min (m <sup>2</sup> )	A. max (km <sup>2</sup> )	A. med (km <sup>2</sup> )	A. tot (km <sup>2</sup> )	N. description (#)	N. description checked (#)	A. description checked (%)	A. min checked (%)
<i>Sr</i>	13,040	50	1909.83	1.32	17,296.50	436	93	90	0.18
<i>Nsr</i>	14,595	263	994.09	0.64	9351.25	382	100	90	0.17
<i>Ir</i>	11074	56	4238.05	0.97	10,778.27	363	55	90	0.22
<i>Pr</i>	5508	239	2447.07	1.66	9121.65	360	112	90	0.18
<i>Lb</i>	7735	259	1227.15	0.81	6256.87	336	85	90	0.21
<i>Cr</i>	21,070	16	4836.92	2.15	45,329.81	1155	304	90	0.05
<i>M</i>	8541	23	243.65	0.70	5964.80	235	78	90	0.21
<i>SM</i>	5382	216	921.16	1.57	8455.40	181	66	90	0.35
<i>Cm</i>	4167	58	911.52	1.62	6752.96	114	25	90	0.67
<i>Ssr</i>	11,930	24	3924.31	2.86	34,099.68	560	145	90	0.12
<i>E</i>	2634	989	238.72	0.70	1839.48	87	22	90	0.72
<i>Ucr</i>	37,641	32	1260.33	1.22	45,764.12	856	229	90	0.08
<i>Ccr</i>	8391	39	1392.17	1.66	13,915.05	397	112	90	0.16
<i>Gd</i>	11337	2145	318.28	0.74	8406.20	107	16	90	0.63
<i>Mw</i>	1231	33	9.18	0.26	315.72	26	26	100	0.02
<i>Ad</i>	125	1573	25.31	0.71	88.72	12	12	100	0.03
<i>Li</i>	329	1252	367.79	4.52	1485.44	10	10	100	0.01
<i>B</i>	968	136	105.96	1.01	978.80	79	35	90	0.60
<i>Al</i>	14,804	66	46,634.58	5.09	75,424.36	583	177	90	0.10



251

252 **Table 3:** Descriptive statistics of the 19 lithological classes. In the left half of the table, the number of polygons, and their minimum,  
253 maximum, average and total area for each lithological class are shown. The right half of the table shows the number of total unique  
254 descriptions and those checked during the technical validation in relation to the percentage of the area covered by the validation (% of the  
255 total area) and the detail of the validation (minimum area checked)

#### 256 **4 Results**

257 The main results of this work are: (i) the translation of the rock type information extracted from the stratigraphic units of the  
258 geological maps of Italy at 1:100,000 scale into lithological classes and (ii) the development of a data architecture open to  
259 further improvement, aimed in particular at linking the lithological classes to their expected geotechnical behaviour.

260 The new *Lithological map of Italy* represents the first freely downloadable national distribution of the different lithological  
261 classes at a high resolution. The map scale is at 1:100,000. The assembled map consists of a total of 180,503 polygons  
262 distributed in 19 lithological classes (Figure 5).

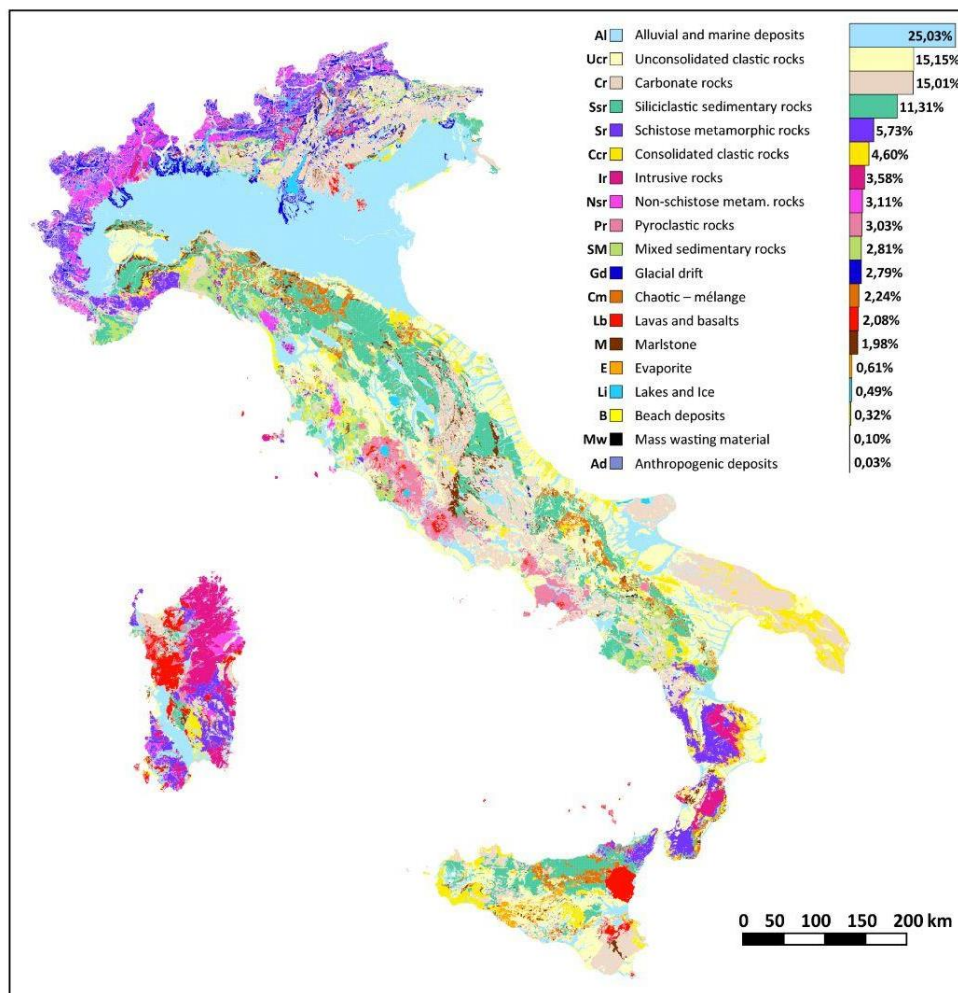


**Figure 5:** Map of Italy showing the 19 lithological classes identified both with the short ID and the extended name. Percentage distribution of each lithological class over the Italian territory is indicated and visualized in a bar chart.

263  
264  
265  
266  
267  
268  
269  
270  
271

The Italian surface is covered by 82,47% sediments (a third of which are alluvial deposits), 8,84% metamorphics, 3,58% plutonics, and 5,11% volcanics (Table 4). A specific class was assigned to areas of ice and inland water bodies, which cover 0,49% of the map area.

Physiographic regions of Italy		Metamorphic		Magmatic			Sedimentary											← I level			
Acronym	Name	Substratum		Intrusion	Cover		Substratum					Undifferentiated Cover					Alluvial/ Marine			← II level	
		Sr	Nsr		Pr	Lb	Cr	M	SM	Cm	Ssr	E	Ucr	Cr	Gd	Mw	Ad	Li	B	Al	← III level
EAL	Eastern Alps	1.7	0.2	0.9	4.0	2.7	46.5	2.2	5.7	-	4.5	0.1	10.3	1.4	9.7	0.3	-	-	0.7	9.3	100



CAL	Central Alps	15.8	13.8	4.5	1.7	0.6	21.1	1.0	3.2	-	2.4	0.0	10.3	0.5	15.8	0.3	-	-	2.7	6.2	100	
WAL	Western Alps	26.7	25.2	4.9	0.1	0.1	6.4	0.5	3.1	0.0	4.8	0.0	8.3	2.1	11.0	0.0	0.0	-	0.7	6.0	100	
PP	Po Plain	0.0	0.1	0.1	0.2	0.1	0.2	0.1	-	0.0	0.4	0.0	1.7	0.4	3.6	-	0.2	0.0	0.5	92.5	100	
NAP	Northern Apennine	1.0	1.5	0.2	-	0.0	6.7	5.6	9.6	10.2	39.0	0.7	11.3	3.3	0.3	0.2	0.0	-	-	10.3	100	
NIAP	North-Internal Apennine	0.7	1.3	0.6	1.7	0.3	6.1	1.3	8.9	1.1	18.6	0.4	28.2	4.8	-	0.1	1.5	0.1	0.6	23.7	100	
CEAP	Centre-Eastern Apennine	-	-	-	-	-	1.0	0.6	-	0.1	12.0	0.3	51.1	11.2	-	0.0	0.5	-	-	23.2	100	
CAP	Central Apennine	-	-	-	3.1	0.1	47.6	9.4	0.0	0.0	14.7	0.0	11.4	2.2	0.4	0.0	0.0	0.0	0.1	10.9	100	
CMP	Central Magmatic Province	0.0	-	-	58.4	9.3	3.4	0.1	0.4	-	0.2	0.0	13.0	0.8	-	0.0	0.0	0.0	3.0	11.3	100	
SMP	Southern Magmatic Province	-	-	-	50.1	3.8	10.3	0.0	-	0.1	3.9	-	21.9	0.0	-	-	1.5	1.6	0.1	6.6	100	
SAP	Southern Apennine	1.8	0.1	0.0	1.9	0.1	20.0	1.5	5.8	7.4	24.8	0.1	21.9	5.9	0.0	0.6	0.1	-	0.0	8.0	100	
SEAP	South-Eastern Apennine	-	-	-	-	-	1.3	0.0	0.0	0.3	0.3	0.0	51.6	7.8	-	0.0	1.1	-	0.6	36.9	100	
GF	Gargano Foreland	-	-	-	-	-	79.3	-	-	-	-	-	4.8	0.3	-	-	0.4	-	3.8	11.4	100	
MF	Murge Foreland	-	-	-	-	-	59.7	-	-	-	-	-	12.1	24.4	-	-	0.2	-	-	3.6	100	
WS	Western Sicily	0.1	-	-	0.0	0.0	10.0	2.5	0.4	7.0	26.6	6.5	24.1	13.6	-	0.0	0.1	-	0.0	9.0	100	
ES	Eastern Sicily	-	-	-	2.8	21.8	27.1	2.4	-	0.5	1.7	0.9	25.0	3.5	-	-	0.3	-	-	14.1	100	
CPA	Calabro-Peloritano Arc	29.0	0.2	14.4	0.3	0.3	2.4	2.7	0.0	2.3	4.8	2.2	22.2	9.0	-	0.0	-	-	-	10.3	100	
SB	Sardinian Block	15.7	5.6	26.6	4.3	13.5	7.0	0.9	-	0.0	3.2	-	3.2	2.8	-	-	0.6	0.0	0.1	16.5	100	
Total Italian territory III level →		5,73	3,11	3,58	3,03	2,08	15,01	1,98	2,81	2,24	11,31	0,61	15,15	4,60	2,79	0,10	0,03	0,49	0,32	25,03	100	
Total Italian territory II level →		8,84	3,58	5,11	33,35							23,28					25,84					100
Total Italian territory I level →		8,84	6,69	82,47																	100	

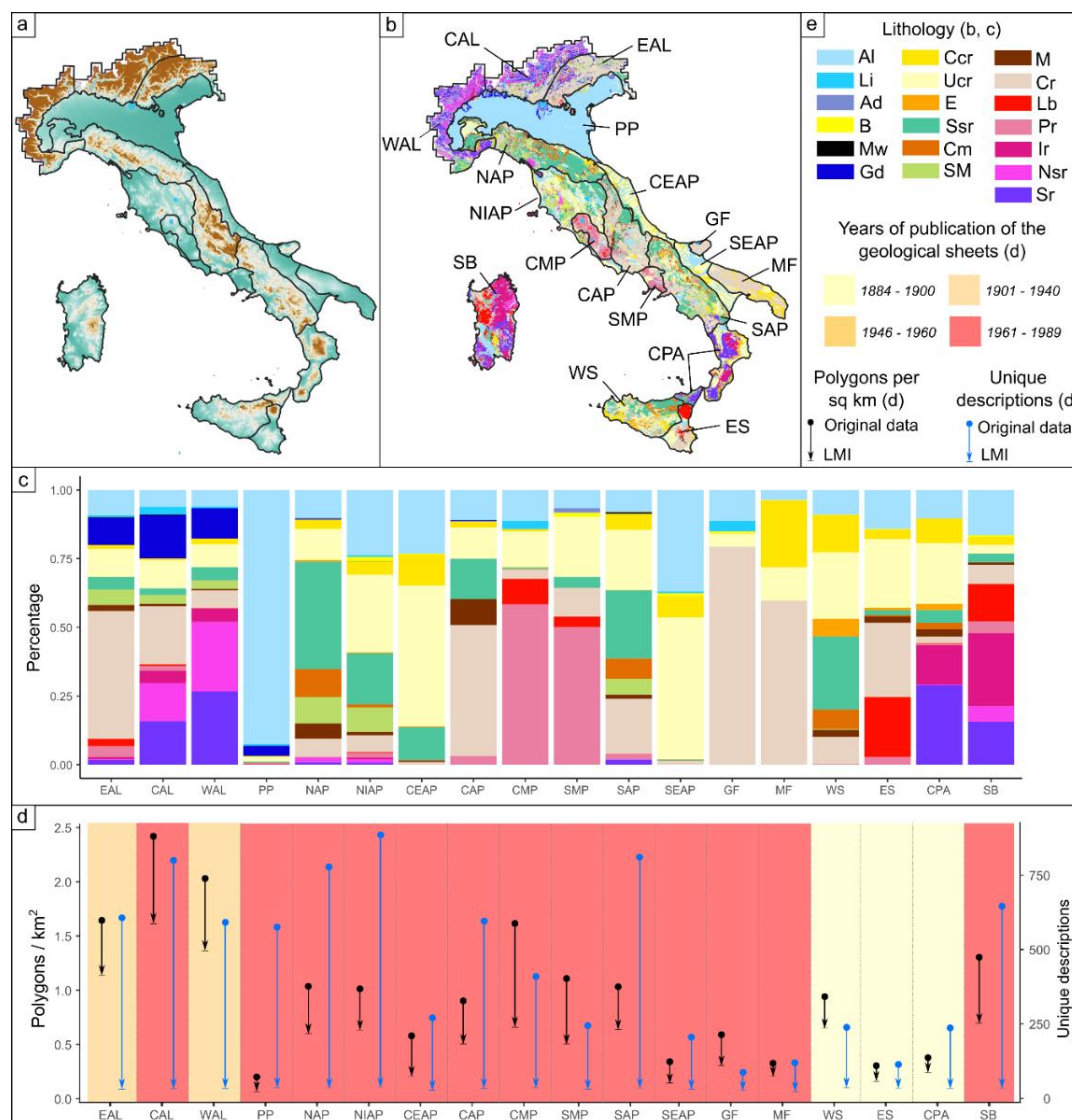
**Table 4:** Percentage distribution of the lithological classes (columns), organized in three hierarchically different levels of classifications, within the 18 physiographic regions of Italy (rows).

Below, the lithological classification describes the general rock types in each unit, in alphabetic order.

- **Alluvial deposits (Al):** alluvial, lacustrine, swamp and marine deposits. Eluvial and colluvial deposits.
- **Anthropogenic deposits (Ad):** include Roman and modern landfills, drainage channel excavations and archaeological remains.
- **Beaches and coastal deposits (B):** include beaches and coastal deposits.
- **Carbonate rocks (Cr):** carbonate-dominant sedimentary rocks. Examples of Cr units are limestone, dolomite and marl (but only where associated and in a clear minority with respect to limestone, otherwise they are included in class M). As usually the rock descriptions of the mapped units do not give relative abundances of the rock types which they encompass, units were classed as Cr if the first named rock type was a carbonate rock, if the majority of rock types were carbonates or if the named order otherwise led to the impression of a domination by carbonates.
- **Chaotic – mélangé (Cm):** include chaotic terrains with a predominantly clay matrix and olistostromes composed by mixed sedimentary rocks (SM class). Fragments of ophiolite structures can be locally included in the Cm class.
- **Consolidated clastic rocks (Ccr):** clay, sand, debris, conglomerates with a varied origin, usually of Neogene and Quaternary age, which have undergone consolidation or secondary cementation phenomena.
- **Evaporite (E):** contains substantial amounts of evaporitic rocks. The typical encountered evaporite rock was gypsum, but also anhydrite and halite. If a map unit was interpreted as dominated by evaporites, it was classified as E, regardless of other mentioned rocks. This implies that E class may additionally contain, e.g., carbonates.
- **Glacial drift (Gd):** include moraines and other related deposits.



- 292 • **Intrusive rocks (Ir):** acid (granites, quartz-diorites, quartz-monzonites), intermediate (diorite, monzonite, syenite),  
293 and basic (gabbros and peridotites) plutonics. Ophiolite structures are included into basic plutonic except for basalt (Lb class)  
294 and serpentinite (Sr class).
- 295 • **Lakes and Ice (Li):** lakes, rivers, ice and glaciers on some Alpine mountains. However, the coverage is not  
296 representative for a lake or ice extent, as the priority of this map is on lithology.
- 297 • **Lavas and basalts (Lb):** volcanic rocks including acid (rhyolites, trachytes or dacites), intermediate (andesites) and  
298 basic (basalt-type rocks, tephrites, tholeites and lamprophyres) volcanics.
- 299 • **Marlstone (M):** includes mostly marly rocks with a composition ranging from calcareous marls to clayey limestones.  
300 Typically, it contains marly sediments of cartographic importance associated with Carbonatic rocks (Cr) or Siliciclastic  
301 sedimentary rocks (Ssr).
- 302 • **Mass wasting material (Mw):** include landslides.
- 303 • **Mixed sedimentary rocks (SM):** sediments where carbonate is mentioned but not dominant. The class encompasses  
304 mixed sedimentary rocks that are usually a combination of different rock types (e.g., interlayered sandstone and limestone, or  
305 shaley marl with interlayered subordinated calcilutite beds or radiolarite). Mixed pelagic sediments as well as calcareous  
306 turbidites are included in the SM class.
- 307 • **Non-schistose metamorphic rocks (Nsr):** metamorphics where schistose fabric can be present but not dominant. It  
308 contains gneiss, amphibolite, quartzite, meta-conglomerate, and marble.
- 309 • **Pyroclastic rocks (Pr):** sediments of volcanic origin. Typical pyroclastics are tuff, volcanic breccias, ash, slag,  
310 pozzolane, pumice.
- 311 • **Schistose metamorphic rocks (Sr):** ‘broad’ lithological class that encompasses a wide variety of rocks from fillade  
312 to schist, including association of schist and paragneiss. Ophiolite derived rocks that show a certain degree of metamorphism  
313 and schistosity (e.g. Serpentinite) are included in this class
- 314 • **Siliciclastic sedimentary rocks (Ssr):** sandstone, mudstone and greywacke. Where carbonate was named in the rock  
315 description of the mapped unit, the lithological classes Cr or SM was used, so siliciclastic sedimentary rocks are without  
316 mapped carbonate influence. Note that in some cases the carbonate presence (e.g., as matrix) may not be named in the rock  
317 description, and siliciclastic sediments may still contain carbonate in nature.
- 318 • **Unconsolidated clastic rock (Ucr):** young, not yet consolidated and/or weathered sediments, usually of Neogene  
319 and Quaternary age. It comprises all grain sizes with a heterogeneous origin loosely arranged and not cemented together.  
320 Examples of unconsolidated sediments are clay soil, sand, not cemented breccia, loose debris and conglomerate.  
321 Significant regional differences in the distribution of lithologies exist (Figure 6a,b,c, Table 4).



322

323 **Figure 6:** (a) Physical map of Italy subdivided into 18 physiographic regions; (b) Geographical distribution of the identified 19 lithological  
 324 classes in the 18 physiographic regions of Italy (see Table 4 for spelling out the acronyms); (c) Percentage distribution of the 19 lithological  
 325 classes in each physiographic region; (d) Polygons density (black symbols) and number of unique description (blue symbols) in each  
 326 physiographic region considering the original data (points) and the LMI (arrow tips), and taking into account the years of publication of the  
 327 geological sheets; (e) Legend. See Figure 5 for the extended lithological legend.

328

329

330 With the exception of flat and low-lying areas of Italy, where alluvial deposits and loose clastic deposits dominate (e.g. Po  
 331 Plain, PP), the map shows a high regional lithological variability. In the Western Alps (WAL) metamorphic rocks dominate  
 332 while in the Eastern Alps (EAL) carbonate rocks prevail. Intermediate percentages are recorded in the Central Alps (CAL),



333 where the metamorphic rocks at N-NW and the sedimentary rocks at S-SE are separated by an important tectonic lineament.  
334 The northern Apennines (NAP) are mainly composed of siliciclastic rocks, and subordinately of chaotic and mixed sedimentary  
335 rocks, while the central Apennines (CAP) consist mainly of carbonate rocks. Intermediate percentages of carbonate rocks,  
336 mixed and chaotic sedimentary rocks, and siliciclastic deposits are found in the North Internal Apennines (NIAP), in the  
337 Southern Apennines (SEAP) and in the Western Sicily (WS). In WS significant percentages of evaporites are also recorded.  
338 In the Central and South Eastern Apennines (CEAP and SEAP), high percentages of unconsolidated and consolidated clastic  
339 rocks are present, while carbonate rocks dominate the lithology of the Gargano and the Murge Foreland (GF and MF). The  
340 similarity between the most represented lithological classes in the Calabro-Peloritano Arc (CPA) and Sardinian Block (SB) is  
341 evident, although schistose rocks prevail in CPA while intrusive rocks prevail in SB. Volcanic rocks are extensively  
342 represented in the Central and Southern Magmatic Province (CMP and SMP), in the Eastern Sicily (ES), in the Sardinian Block  
343 (SB), and subordinately in the Eastern Alps (EAL).

344 Significant regional differences in the representation of lithologies also exist (Figure 6d). In the original geological dataset, the  
345 number of polygons per squared kilometres (black points in Figure 6d) used to represent the lithological variability is strongly  
346 heterogeneous across Italy, and is proportional to the geo-lithological complexity of each physiographic region. For instance,  
347 the Alpine regions (EAL, CAL, WA), which are characterized by a complex geological architecture and by a very high  
348 lithological variability, display the higher polygon density, with values between 1.7 e 2.4 polygons/km<sup>2</sup>. On the other hand,  
349 the Po Plain (PP) records the lowest polygons density, with 0,2 polygons per square kilometre, being characterized by a quite  
350 monotonous surface geology, almost totally represented by alluvial deposits. Accordingly, in the Apennine regions, which are  
351 (in general) geologically less complex than the Alpine regions, the average polygon density is just over 1 (NAP, NIAP, CAP,  
352 SMP, SAP) with a maximum of 1,7 in the Central Magmatic Province (CMP) and a minimum of 0,3 in the south-eastern  
353 regions of the foredeep (SEAP) and foreland (MF) domains.

354 The reclassification of the original geological dataset in the LMI classes determined the merging of adjacent polygons exposing  
355 rock unit included in the same lithological class. The process resulted in a drop of the number of polygons in each physiographic  
356 region, passing from the original data set to the LMI, which is indicated by the length of the black arrows in Figure 6d.  
357 Importantly, the reduction of the number of polygons does not changes the relative regional variability of the polygon density.  
358 This means that the simplification introduced by our reclassification does not impact the regional difference in the  
359 representation of the lithology.

360 In Figure 6d, the indicator of polygon density (in black) is flanked by an analogue indicator (in blue) displaying the count of  
361 the unique descriptions used within each physiographic region, both in the original data set (blue points) and in the reclassified  
362 LMI (blue arrow tips). The number of unique descriptions is generally proportional to the polygon density, but cases of  
363 exceptionally high number of unique descriptions (e.g. PP, NAP, NIAP, SAP) are common. Primarily, this is the effect of



364 individual geologists or working groups using several local names to define the same rock unit, thus increasing the number of  
365 unique descriptions.

366 Finally, Figure 6d shows that regional differences in the representation of lithologies may be also related to the different years  
367 of publication of the geological sheets encompassed in each region. Figure 6d shows that: i) the geological sheets encompassed  
368 in the Alpine region have been surveyed in the periods 1901-1940 (EAL, WAL) and 1961-1989 (CAL); ii) almost all the  
369 geological sheets encompassed in the regions of the Italian Peninsula (PP, NAP, NIAP, CEAP, CAP, CMP, SMP, SAP, SEAP,  
370 GF, MF) have been surveyed in the period 1961-1989, as those of the Sardinian Block (SB); iii) the geological sheets of  
371 Western Sicily (WS) Eastern Sicily (ES) and Calabro Peloritano Arc (CPA) have been surveyed in the period 1884-1900.  
372 While it is not clear whether the publication year of the geological sheets plays or not a role in controlling the polygon density  
373 in the Alpine regions, the impact of the different years of publications in the representation of the regional lithological  
374 variability is dramatic comparing CPA and SB. In fact, despite a similar lithological composition (Figure 6c) and a pre-Alpine  
375 common geological history (Alvarez and Shimabukuro, 2009), CPA and SB are characterized by a very different density of  
376 polygons (0,3 polygons/km<sup>2</sup> for CPA, and 1,3 for SB), due to strong differences in drafting geological sheets published almost  
377 100 years apart from each other.

## 378 **5 Discussions**

379 The main challenge in developing a categorized lithological map lies in balancing accuracy and complexity and still properly  
380 representing the diversity of lithological variables using a limited yet reasonable number of classes, to ensure ready  
381 interpretation and applicability of the map. We maintain that the 19 classes defined here allow to optimize the use of the map  
382 for several applications, with a focus on landslides modelling. Despite the specific goals of this work, we applied a  
383 classification that can be reconciled with the ones adopted in global lithological databases (Table 1; Hartmann et al., 2012;  
384 Geological Survey of Canada, 1995), emphasizing the dominant rock types. Furthermore, information on the physical  
385 characteristics of the dominant rock types available in the original geological legend were used to define specific lithological  
386 classes.

387 For example, metamorphic rocks were split in two broad classes considering the dominant presence of schistose or not schistose  
388 rocks, hence according to expected - or not expected - pervasive planar anisotropies within the rock bodies. Similarly, the  
389 classes of consolidated and unconsolidated clastic sediments, in our map, consist of two separate classes, according to their  
390 expected different geotechnical behaviour. In both cases, differences in physical features (*e.g.* schistose/non-schistose,  
391 consolidated/unconsolidated) may impact landslide susceptibility of genetically similar rocks (Bucci et al., 2016b), hence  
392 justifying the need of these lithological classes for our scope.

393 We also included the class Marlstone, quite unusual for generalized lithological characterization at national scale. The need of  
394 this class derives from the systematic occurrence of significant marls interbeds within carbonate or siliciclastic rocks, whose



395 representation highlights the cartographic detail of the map. Moreover, it is widely recognized that marls intercalations  
 396 represent important geo-hydrological and mechanical discontinuities within rocks bodies, often promoting landslide  
 397 phenomena (Guzzetti et al., 1996), which is a relevant issue for our purpose. As our map is designed to be used for landslides  
 398 studies and modelling, we also decided to maintain the class “landslides”, although it covers only 0,1% of the Italian territory.  
 399 We are aware that this percentage value is strongly underestimated. The Inventory of Italian Landslides (Trigila et al., 2010),  
 400 still incomplete, counts over 620,000 landslides covering a total area equal to 7.9% of the Italian territory, and occurrence of  
 401 the different types of landslides gives rise to very different patterns of landslide susceptibility, consistently with the diverse  
 402 lithological formations (Lombardo et al., 2021). However, we acknowledge that the large difference in percentage values  
 403 stems from the fact that many efforts in landslide mapping have been made in recent decades, when the 277 sheets of the  
 404 geological map of Italy at 1: 100,000 scale were already published.

405 Despite the usage of very specific lithological classes helps a reliable classification of the rock types, the map is still subject  
 406 to uncertainty considering rock properties of some broad lithological classes. This is highlighted, for instance, by the  
 407 considerable amount of mixed limestone, marls and shale sediments (5%), including the Chaotic (2.2%) and the Mixed  
 408 sedimentary (2.8%) classes. Despite carbonate rocks and siliciclastic rocks behave differently for a large range of physical or  
 409 chemical properties (*e.g.*, weathering processes, dissolution rates or aquifer characteristics), they occur often “mixed” in these  
 410 two geo-lithological classes, further undistinguishable at the scale of the used maps here.

411 An additional source of uncertainty remains at the boundaries of the geological sheets, where only discontinuities between  
 412 contiguous sheets longer than 1 km were resolved, with the exception of 58 segments over the entire national territory. Table  
 413 5 represents a contiguity matrix for these 58 segments. Table 5 reveals that 19 segments, 33% of the total, bound polygons  
 414 pertaining to the Al (Alluvial and marine deposits) class, which is the most represented lithological class at national scale,  
 415 covering the 25% of the entire national territory. The segments that bound lithological classes belonging to the same genetic  
 416 groups (metamorphic, magmatic, sedimentary) are 24, 10 of which separate lithological classes of the sedimentary substratum  
 417 from others belonging to sedimentary covers. Only 15 segments bound lithological classes belonging to different genetic  
 418 groups. Despite all these segments represent identical inconsistencies from a graphical point of view, their potential negative  
 419 local effects on the map reliability may be different from a lithological point of view. For instance, for landslide studies, we  
 420 can consider negligible the potential negative effects of unrealistic, linear lithological boundaries of polygons pertaining to the  
 421 Al class since they cover (almost) only flat areas of fluvial, alluvial and coastal plain, where landslides are unexpected.

422  
423

I level classification →		Metamorphic		Magmatic			Sedimentary													
II level classification →		Metamorphic		Intrusion	Cover		Substratum					Undifferentiated Cover						Alluvial/Marine		
III level classification →		Sr	Nsr	Ir	Pr	Lb	Cr	M	SM	Cm	Ssr	E	Ucr	Ccr	Gd	Mw	Ad	Li	B	Al
Metamorphic	Sr	0	3	2	0	0	2	0	0	0	1	0	3	1	2	0	0	0	0	1
	Nsr	3	0	1	0	0	0	0	0	0	0	0	0	1	0	0	0	0	0	2
Magmatic	Ir	2	1	0	1	0	0	0	0	0	0	0	0	0	0	0	0	0	0	4
	Pr	0	0	1	0	0	0	0	0	0	0	0	1	0	1	0	0	0	0	1



Sedimentary substratum	Lb	0	0	0	0	0	0	0	0	0	0	0	0	0	0	0	0	0	0	0
	Cr	2	0	0	0	0	0	1	0	0	2	0	3	2	0	0	0	0	0	1
	M	0	0	0	0	0	1	0	0	0	3	0	0	0	0	0	0	0	0	1
	SM	0	0	0	0	0	0	0	0	0	0	0	1	0	0	0	0	0	0	0
	Cm	0	0	0	0	0	0	0	0	0	1	0	0	0	0	0	0	0	0	1
	Ssr	1	0	0	0	0	2	3	0	1	0	0	2	2	0	0	0	0	0	2
Undifferentiated sedimentary cover	E	0	0	0	0	0	0	0	0	0	0	0	0	0	0	0	0	0	1	
	Ucr	3	0	0	1	0	3	0	1	0	2	0	0	3	0	0	0	0	0	
	Cer	1	0	0	0	0	2	0	0	0	2	0	3	0	0	0	0	0	2	
	Gd	2	1	0	1	0	0	0	0	0	0	0	0	0	0	0	0	0	2	
	Mw	0	0	0	0	0	0	0	0	0	0	0	0	0	0	0	0	0	0	
	Ad	0	0	0	0	0	0	0	0	0	0	0	0	0	0	0	0	0	0	
	Li	0	0	0	0	0	0	0	0	0	0	0	0	0	0	0	0	0	0	
Alluvial/Marine	B	0	0	0	0	0	0	0	0	0	0	0	0	0	0	0	0	0	1	
	Al	1	2	4	1	0	1	1	0	1	2	1	0	2	2	0	0	0	1	
Total number →		15	7	8	4	0	11	5	1	2	13	1	13	10	6	0	0	0	19	

424

425 **Table 5:** Contiguity matrix showing the number of the 58 N-S and E-W oriented straight segments longer than 1000 m which bounds each  
 426 lithological class.

427

428 On the other hand, critical differences remain between rocks pertaining to the same genetic group but characterized by different  
 429 physical properties (schistose/non schistose metamorphic rocks, consolidated/unconsolidated sedimentary clastic rocks).  
 430 Overall, we consider as resolved the inhomogeneity problems at the boundaries between adjacent geological sheets for  
 431 segments equal to or greater than 1000 meters, hence considering the remaining 58 segments longer than 1000 meters listed  
 432 in Table 1 as acceptable and/or negligible exceptions. Since in cartography the admissible error is traditionally assumed to be  
 433 1 mm, we maintain that, only along the boundaries of the geological sheets our map is formally correct at the scale of  
 434 1:1,000,000, while elsewhere the cartographic detail remains compatible with the scale 1:100,000. Pushing harmonization  
 435 operation into more detail would require altering the original data, which is outside the scope of this work.

436 The design of the LMI allows for further corrections and inclusion of additional information, (*e.g.*, age information, tectonic  
 437 history, geotechnical properties, fine-coarse grain size ratio) in future versions, customizable for different usage, with expected  
 438 reduction of general and/or specific uncertainties. Additional information may be organized into more detailed classification  
 439 levels, although their compilation will require further efforts to collect data from local geo-lithological literature and site-  
 440 specific investigations.

441 Since different purposes impose different generalizations strategies, other lithological classifications of the Italian rocks are  
 442 possible, starting from the same source dataset. For instance, aiming at a seismic soil classification of Italy, Forte et al. (2019)  
 443 generalized the lithology of Italy using 20 classes, a number comparable to the 19 classes presented here. In their classification,  
 444 a relevant distinction was based on the identification of geo-lithological complexes as geologic bedrock, versus those  
 445 representative of cover deposits, being the last category directly related to defined values of  $V_s$  (average speed of propagation  
 446 of shear waves), hence particularly relevant for their purpose. On the other hand, the most recent lithological map of Italy  
 447 provided by ISPRA as a web service is accompanied by a complex legend, articulated in 48 classes aimed at describe age,  
 448 genesis and chemical-physical characteristics of rocks, focusing on a comprehensive geological rock characterization, without  
 449 specific applicative purpose. It is evident that different classifications allow different possible usages of the same original

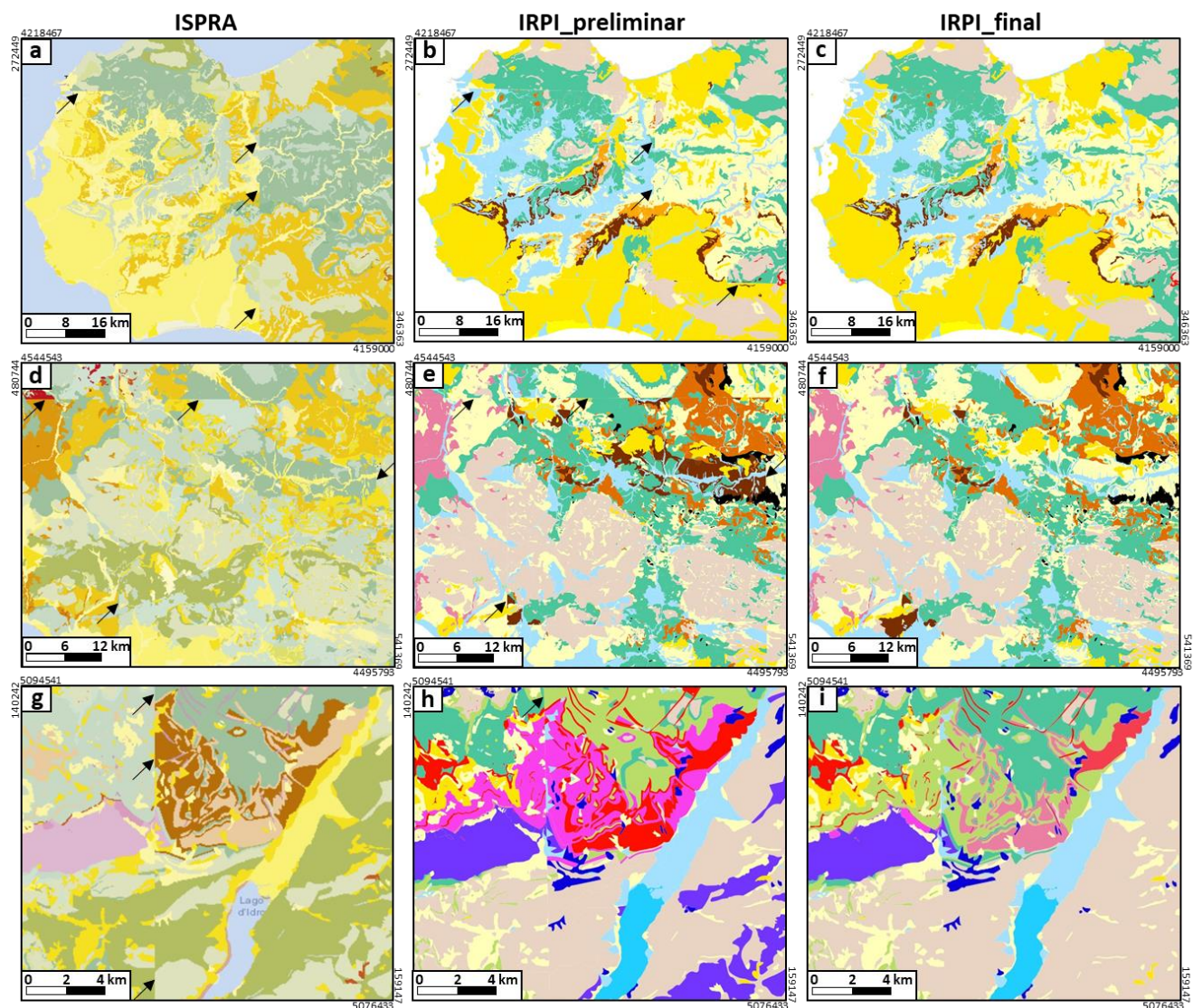


450 dataset, hence, at the same representation scale, different lithological characterizations can be more or less suitable depending  
451 on the intended purpose.

452 Although the general rock composition of the Italian's surface is remarkably similar between the existing digital lithological  
453 maps (Table 1, ID 5) the representation of the rock distribution varies largely between them, and have been greatly improved  
454 in the present map, especially across geological sheets. Compared to smaller-scale maps (Compagnoni et al., 1976-1983), the  
455 main improvements lays in a better representation of complex geological settings. Moreover, a better lithological  
456 harmonization along the borders of the original geological sheets distinguishes our map from other maps at the same scale  
457 (Servizio Geologico d'Italia, 2004). Figure 7 shows examples for Sicilia, Campania and Lombardia regions, highlighting the  
458 general improvement of the map, regardless of the geographical location, geological and geomorphological settings. However,  
459 a direct comparison of the maps is difficult due to the different legends (*e.g.* based on geological processes or lithology, or  
460 mixing up processes and lithology).

461 Early versions of the LMI presented here were already used to validate terrain classification of Italy (Alvioli et al., 2020) and  
462 to estimate soil parameters for physically based rockfall modelling along the Italian railway (Alvioli et al., 2021). Such versions  
463 of the map included a few of the inconsistencies resolved in this work. We expect that a similar use of the map could be  
464 extended to study and model other types of landslides in different lithological settings, both widespread in the landscape and  
465 along specific infrastructure networks.

466



467

468 **Figure 7:** Comparison of two different classifications of the same source dataset for selected areas of Sicilia (a, b, c), Campania (d, e, f) and  
469 Lombardia (g, h, i) regions. Examples from the lithological map of Italy according to ISPRA classification as visualized in vector form at  
470 the ISPRA website (URL in Table 1, ID 5) are shown in (a), (d) and (g). For the same areas, the lithological map of Italy according to our  
471 own preliminar semi-automatic classification partially resolved the major inconsistencies along the boundaries of the geological sheets  
472 already present in (a), (d) and (g), even if critical boundaries still remains, see black arrows as reference; Most of the inconsistencies were  
473 resolved manually by expert analysis in the final version of our map (c, f, i) leading a substantial improvement of the lithological  
474 harmonization along the borders of the original geological sheets.

475

476



## 477 **6 Conclusions**

478 This paper described the first freely downloadable lithological map of Italy at 1:100.000 scale, providing the distribution of  
479 rock-attributes and rock-types of the Italian territory in digital format.

480 The LMI was assembled from 277 sheets of the geological map of Italy at 1: 100,000 scale and distributed in digital vector  
481 format through a REST service on the ISPRA website. For the purpose, the rock types associated with the 5.456 unique  
482 geological descriptions in the source dataset were identified and translated into the 19 general classes defined here. Adjacent  
483 polygons grouped within the same class were dissolved, reducing their number from the original 292,705 to the 180,503 in the  
484 final product. Most of the work consisted with database queries, coupled with expert analysis of the location of the polygons  
485 using the sheets available at scale 1:50,000 (where present), and with any potentially useful information sought in regional and  
486 local literature. Particular attention was paid to harmonize the lithological information at the boundary of the original  
487 geological sheets. A final technical validation allowed to detect and resolve residual problems, also related to inconsistencies  
488 inherited from the source dataset, and guaranteed the overall quality of the work.

489 The LMI allows the assessment of national scale research questions at high resolution and thus helps to advance our knowledge  
490 on the relationships between lithology and surface processes, including multiple geomorphological, geo-hydrological and  
491 environmental issues. In addition, the resolution of the LMI highlights the differences in the lithological cover of the different  
492 regions and sub-regions, hence facilitating the comparison of results of different regional studies (*e.g.*, susceptibility to  
493 landslides and floods).

494 The map has limits and can be enhanced, in particular in local areas where geo-lithological descriptions in the source dataset  
495 were not exhaustive and our knowledge is limited. Inclusion of more detailed regional maps or other relevant additional  
496 information, *e.g.*, age, tectonic history, geotechnical properties, fine-coarse grain size ratio are out of the aim of this work, but  
497 may be included in future versions. Aware of these and other potential and desirable future upgrades, we provided the LMI  
498 with a very simple and open architecture, which allows more details or levels of information to be added and could thus be  
499 developed further in accordance with specific scientific questions.

## 500 **7 Data availability**

501 The digital lithological Map of Italy at 1:100.000 is provided in the PANGAEA database.  
502 <https://www.pangaea.de/tok/14419d5a5f6846ed4471505ea29d94a414e37714> (Bucci et al. 2021).

## 503 **8 Contributions**

504 Francesco Bucci (FB), Michele Santangelo (MS), Lorenzo Fongo (LF), Mauro Cardinali (MC) and Ivan Marchesini (IM)  
505 decided the classification system, performed multiscale comparative analysis, and drafted the final version of the lithological



506 map. Ivan Marchesini (IM) e Massimiliano Alvioli (MA) prepared the dataset and the script for the final classification. FB,  
507 MS, LF, MC, IM and Laura Meelli (LM) compiled the Legend and designed the layout of the final map. FB, MS wrote the  
508 text. LF, MC, IM, MA, LM reviewed and integrated the paper at several stages, IM supervised the research activity.

## 509 **9 Acknowledgements**

510 The work was partly carried out within the FRA.SI (Multi-scale integrated methodologies for seismically-induced landslides  
511 risk zonation) project, of the National Research council of Italy (CNR).

## 512 **References**

- 513 Alvarez, W., Shimabukuro D.H.: The geological relationships between Sardinia and Calabria during Alpine and Hercynian  
514 times. *Italian Journal of Geosciences*, 128, 2, 257–268. doi: <https://doi.org/10.3301/IJG.2009.128.2.257>, 2009.
- 515 Alvioli, M., Guzzetti, F., Marchesini, I.: Parameter-free delineation of slope units and terrain subdivision of Italy,  
516 *Geomorphology*, 358, 107-124. <https://doi.org/10.1016/j.geomorph.2020.107124>, 2020.
- 517 Alvioli, M., Marchesini, I., Reichenbach, P., Rossi, M., Ardizzone, F., Fiorucci, F., Guzzetti, F.: Automatic delineation of  
518 geomorphological slope units and their optimization for landslide susceptibility modelling, *Geosci. Model Dev.* 9,  
519 3975–3991. <https://doi.org/10.5194/gmd-9-3975-2016>, 2016.
- 520 Alvioli, M., Santangelo, M., Fiorucci, F., Cardinali, M., Marchesini, I., Reichenbach, P., Rossi, M., Guzzetti, F., Peruccacci,  
521 S.: Rockfall susceptibility and network-ranked susceptibility along the Italian railway. *Engineering Geology*, 2021 (in  
522 press).
- 523 Amanti, M., Battaglini, L., Campo, V., Cipolloni, C., Congi, M.P., Conte, G., Delogu, D., Ventura, R., Zonetti, C.: The  
524 Lithological map of Italy at 1:100.000 scale: An example of re-use of an existing paper geological map. In: 33rd  
525 International Geological Conference, IEI02310L - 6-14th August, Oslo (Norway), 2008.
- 526 Amanti, M., Battaglini, L., Campo, V., Cipolloni, C., Congi, M.P., Conte, G., Delogu, D., Ventura, R., Zonetti, C.: La carta  
527 litologica d'italia alla scala 1:100.000. *Atti della 11a Conferenza Nazionale ASITA, Centro Congressi Lingotto, Torino,*  
528 6–9 Novembre 2007, <http://atti.asita.it/Asita2007/Pdf/119.pdf>, 2007.
- 529 Amodio Morelli, L., Bonardi, G., Colonna, V., Dietrich, D., Giunta G., Liguori, V., Lorenzoni, S., Paglianico, A., Perrone, V.,  
530 Piccarreta, G., Russo, M., Scandone, P., Zanettin, E., Zuppetta, A.: L'arco Calabro Peloritano nell'Orogene  
531 Appenninico-Magrebide, *Memorie della Società Geologica Italiana*, 17, 1-60, 1976.
- 532 Asch, K.: The 1:5 million international geological map of Europe and adjacent areas. *Bundesanstalt für Geowissenschaften  
533 und Rohstoffe, Commission of the Geological Map of the World, Subcommittee for Europe. BGR, Hannover, 2005.*



- 534 Bentivenga, M., Coltorti, M., Prosser, G., Tavarnelli, E.: Deformazioni distensive recenti nell'entroterra del Golfo di Taranto:  
535 implicazioni per la realizzazione di un deposito geologico per scorie nucleari nei pressi di Scanzano Jonico (Basilicata),  
536 Boll. Soc. Geol. It., 123, 3, 391-404, 2004.
- 537 Boni, C.F., Bono, P., Funicello, R., Parotto, M., Praturlon, A., Fanelli, M.: Carta delle manifestazioni termali e dei complessi  
538 idrogeologici, scala 1:1.000.000. In: Contributo alla conoscenza delle risorse geotermiche del territorio italiano. CNR,  
539 Progetto Finalizzato Energetica, Sottoprogetto Energia Geotermica, Roma, 1984.
- 540 Bonomo, R., Capotorti, F., D'Ambrogi, C., Di Stefano, R., Graziano, R., Martarelli, L., Pampaloni, M.L., Pantaloni, M., Ricci,  
541 V., Compagnoni, B., Galluzzo, F., Tacchia, D., Masella, G., Pannuti, V., Ventura, R., Vitale, V.: Carta geologica d'Italia  
542 alla scala 1:1.250.000, Serv. Geol. d'It., APAT, Roma, 2005.
- 543 Bortolotti, V., Fazzuoli, M., Pandelli, E., Principi, G., Babbini, A., Corti, S.: Geology of Central and Eastern Elba Island, Italy,  
544 Ofioliti, 26(2): 97-150, 2001.
- 545 Brogi, A., Liotta, D.: Fluid flow paths in fossil and active geothermal fields: the Plio-Pleistocene Boccheggiano-Montieri and  
546 the Larderello areas, Geological Field Trips of the Italian Geological Society, vol. 3(2.2), ISSN: 2038- 4947,  
547 doi:10.3301/GFT.2011.03, 2011.
- 548 Brozzetti, F.: Geological map (1: 25.000 scale) of the Northern Umbria Preapennines in the M:S:M: Tiberina area (Umbria  
549 Italy). Boll. Soc. Geol. It, 126, 511-529, 2007.
- 550 Bucci, F., Novellino, R., Guglielmi, P., Prosser, G., & Tavarnelli, E. (2012). Geological map of the northeastern sector of the  
551 high Agri Valley, Southern Apennines (Basilicata, Italy). Journal of Maps, 8, 282–292.  
552 <https://doi.org/10.1080/17445647.2012.722403>
- 553 Bucci, F., Novellino, R., Tavarnelli, E., Prosser, G., Guzzetti, F., Cardinali, M., Gueguen, E., Guglielmi, P., Adurno, I.: Frontal  
554 collapse during thrust propagation in mountain belts: a case study in the Lucania Apennines, Southern Italy, J. Geol.  
555 Soc. 171, 571–581, <https://doi.org/10.1144/jgs2013-103>, 2014.
- 556 Bucci, F., Mirabella, F., Santangelo, M., Cardinali, M., Guzzetti, F.: Photo-geology of the Montefalco Quaternary Basin,  
557 Umbria, Central Italy, Journal of Maps 12:314–322, <https://doi.org/10.1080/17445647.2016.1210042>, 2016a.
- 558 Bucci, F., Santangelo, M., Cardinali, M., Fiorucci, F., Guzzetti, F.: Landslide distribution and size in response to Quaternary  
559 fault activity: the Peloritani Range, NE Sicily, Italy, Earth Surf. Process. Landf. 41, 711–720,  
560 <https://doi.org/10.1002/esp.3898>, 2016b.
- 561 Bucci, F., Tavarnelli, E., Novellino, R., Palladino, G., Guglielmi, P., Laurita, S., Prosser, G., Bentivenga, M.: The History of  
562 the Southern Apennines of Italy Preserved in the Geosites Along a Geological Itinerary in the High Agri Valley,  
563 Geoheritage 11, 1489–1508, <https://doi.org/10.1007/s12371-019-00385-y>, 2019.
- 564 Bucci, F., Novellino, R., Guglielmi, P., Tavarnelli, E.: Growth and dissection of a fold and thrust belt: the geological record  
565 of the High Agri Valley, Italy. J. Maps 16, 245–256, <https://doi.org/10.1080/17445647.2020.1737254>, 2020.



- 566 Bucci, F., Santangelo, M., Fongo, L., Alvioli, M., Cardinali, M., Meelli, L., Marchesini, I.: A new digital lithological Map of  
567 Italy at 1:100.000 scale. PANGAEA, <https://doi.pangaea.de/10.1594/PANGAEA.935673> (dataset in review), 2021.
- 568 Campobasso, C., Salvati, L., Vita, L. Eds.: Evoluzione dei bacini neogenici e loro rapporti con il magmatismo plio-quadernario  
569 dell'area tosco-laziale (Pisa, 1991), Mem. Descr. Carta Geol. d'It., 49, pp. 375, Ser. Geol. d'It., Roma, 1994.
- 570 Carmignani, L., Conti, P., Cornamusini, G., Pirro, A.: Geological map of Tuscany (Italy), *J. Maps* 9, 487–497,  
571 <https://doi.org/10.1080/17445647.2013.820154>, 2013.
- 572 Carmignani, L.: Geologia della Sardegna. Note illustrative della Carta Geologica della Sardegna a scala 1:200.000. Mem.  
573 Descr. Carta Geol. d'It., 60: pp. 283, Serv. Geol. d'It., Roma, 2001.
- 574 Catanzariti, R., Ottria, G., Cerrina Feroni, A.: Carta geologico-strutturale dell'Appennino Emiliano-Romagnolo. Scala  
575 1:250.000. RER - Servizio Geologico, Sismico e dei Suoli; CNR - Istituto di Geoscienze e Georisorse, Pisa, 2002.
- 576 Celico, P.B., De Vita, P., Monacelli, G., Scalise, A.R., Tranfaglia, G.: Carta idrogeologica dell'Italia Meridionale, scala  
577 1:250.000. ISPRA, Roma, 2005.
- 578 Centamore, E., Panbianchi, G., Deiana, G., Calamita, F., Cello, G., Dramis, F., Gentili, B., Nanni, T.: Ambiente fisico delle  
579 Marche. Geologia, Geomorfologia, Idrogeologia alla scala 1:100.000. Regione Marche, 1991.
- 580 Chiarini, E., D'Orefice, M., Graciotti, R.: Le unità stratigrafiche di riferimento nella rappresentazione cartografica dei depositi  
581 plio-quadernari continentali nel Progetto CARG. Esempi: Arco alpino, Pianura Padana e Sardegna. *Il Quaternario*, 21,  
582 1A, 51-56, 2008.
- 583 Cipolloni, C., Pantaloni, M., Ventura, R., Vitale, V., Tacchia, D.: The GEO1MDB: the database of the 1:1,000,000 scale  
584 geological map of Italy. In: 6th EUREGEO Proceeding, 1: 218-221, 2009.
- 585 Compagnoni, B.: La Carta geologica d'Italia, alla scala 1:1.000.000. Mem. Descr. Carta Geol. It., 71, 207-212, 2004.
- 586 Compagnoni, B., Damiani, A.V., Valletta, M.: Carta geologica d'Italia alla scala 1:500.000. In 5 fogli e note illustrative,  
587 Servizio Geologico d'Italia, Roma, 1976-1983.
- 588 Consiglio Nazionale delle Ricerche: Structural model of Italy and gravity map. *Quaderni della Ricerca Scientifica*, 114, 3,  
589 1990.
- 590 Console, F., Pantaloni, M., Petti, F.M., Tacchia, D.: La cartografia del Servizio geologico d'Italia = The Geological survey of  
591 Italy mapping, ISBN:978-88-9311-052-5, 2017.
- 592 Conti, P., Cornamusini, G., Carmignani, L.: An outline of the geology of the Northern Apennines (Italy), with geological map  
593 at 1:250,000 scale, *Ital. J. Geosci.* 139, 149–194, <https://doi.org/10.3301/IJG.2019.25>, 2020.
- 594 Corpo Reale delle Miniere: Carta mineraria d'Italia. Scala 1:500.000, Roma, 1926-1935.
- 595 Coulthard, T.J.: Landscape evolution models: A software review, *Hydrol. Processes*, 15, 1, 165–173, doi:10.1002/hyp.426,  
596 2001.



- 597 D'Ambrogi, C., Scrocca, D., Pantaloni, M., Valeri, V., Doglioni, C.: Exploring Italian geological data in 3D. In: M.  
598 BELTRANDO, A. PECCERILLO, M. MATTEI, S. CONTICELLI & C. DOGLIONI: The Geology of Italy. Journal  
599 of the Virtual Explorer, 36, paper 33. doi:10.3809/jvirtex.2010.00256, 2010.
- 600 De Graaf, I.E.M., Van Beek, R.L.P.H., Gleeson, T., Moosdorf, N., Schmitz, O., Sutanudjaja, E.H., Bierkens, M.F.P.: A global-  
601 scale two-layer transient groundwater model: Development and application to groundwater depletion. Adv. Water  
602 Resour. 102, 53–67. <https://doi.org/10.1016/j.advwatres.2017.01.011>, 2017.
- 603 De Rita D., Fabbrini, M., Cimarelli, C. (2004) - Evoluzione pleistocenica del margine tirrenico dell'Italia centrale tra  
604 eustatismo, vulcanismo e tettonica. *Il Quaternario*, 17(2): 523-536.
- 605 De Sousa, L.M., Poggio, L., Batjes, N.H., Heuvelink, G.B.M., Kempen, B., Riberio, E., Rossiter, D., 2020. SoilGrids 2.0:  
606 producing quality-assessed soil information for the globe. *SOIL Discuss.* 1–37. <https://doi.org/10.5194/soil-2020-65>
- 607 Delogu, D., Campo, V., Cipolloni, C., Congi, M.P., Falcetti, S., Moretti, P. Pampaloni, M. L., Pantaloni, M., Roma, M.,  
608 Ventura, R.: Il Portale del Servizio Geologico d'Italia: uno strumento al servizio dei geologi professionisti. *Professione*  
609 *Geologo*, 32, 4, 24-27, 2012.
- 610 Donnini, M., Marchesini, I., Zucchini, A., 2020a. Geo-LiM: a new geo-lithological map for Central Europe (Germany, France,  
611 Switzerland, Austria, Slovenia, and Northern Italy) as a tool for the estimation of atmospheric CO<sub>2</sub> consumption. *J.*  
612 *Maps* 16, 43–55. <https://doi.org/10.1080/17445647.2019.1692082>
- 613 Donnini, M., Marchesini, I., Zucchini, A., 2020b. A new Alpine geo-lithological map (Alpine-Geo-LiM) and global carbon  
614 cycle implications. *GSA Bull.* 132, 2004–2022. <https://doi.org/10.1130/B35236.1>
- 615 Dürr, H.H., Meybeck, M., Dürr, S.H., 2005. Lithologic composition of the Earth's continental surfaces derived from a new  
616 digital map emphasizing riverine material transfer. *Glob. Biogeochem. Cycles* 19, n/a-n/a.  
617 <https://doi.org/10.1029/2005GB002515>
- 618 Forte, G., Chioccarelli, E., De Falco, M., Cito, P., Santo, A., Iervolino, I., 2019. Seismic soil classification of Italy based on  
619 surface geology and shear-wave velocity measurements. *Soil Dyn. Earthq. Eng.* 122, 79–93.  
620 <https://doi.org/10.1016/j.soildyn.2019.04.002>
- 621 Ge.Mi.Na. (1962). Ligniti e torbe dell'Italia continentale. *Geomineraria nazionale*, 1–319
- 622 Geological Survey of Canada, Open File 2915d, doi:10.4095/195142, 1995, [https://mrddata.usgs.gov/geology/world/map-](https://mrddata.usgs.gov/geology/world/map-us.html#home)  
623 [us.html#home](https://mrddata.usgs.gov/geology/world/map-us.html#home) (access date 2021/05/07)
- 624 Giannandrea, P., La Volpe, L., Principe, C., Schiattarella, M. (2006) - Carta geologica del Monte Vulture. Scala 1:25.000. In:  
625 PRINCIPE C., La geologia del Monte Vulture, CNR, Regione Basilicata. pp. 217.
- 626 Giardino, M. & Fioraso, G. (1998) - Cartografia geologica delle formazioni superficiali in aree di catena montuosa: il  
627 rilevamento del F. "Bardonecchia" nell'ambito del progetto CARG. *Mem. Sci. Geol.*, 50: 133-153



- 628 Gibbs, M.T., Kump, L.R., 1994. Global chemical erosion during the Last Glacial Maximum and the present: Sensitivity to  
629 changes in lithology and hydrology. *Paleoceanography* 9, 529–543. <https://doi.org/10.1029/94PA01009>
- 630 Girotti, O. & Mancini, M. (2003) - Plio-Pleistocene stratigraphy and relations between marine and non-marine successions in  
631 the middle valley of the Tiber river (Latium, Umbria). *Il Quaternario, Italian Journal of Quaternary Sciences*, 16 (1 bis):  
632 89-106.
- 633 Giustini, F., Ciotoli, G., Rinaldini, A., Ruggiero, L., Voltaggio, M.: Mapping the geogenic radon potential and radon risk by  
634 using Empirical Bayesian Kriging regression: A case study from a volcanic area of central Italy, *Science of The Total*  
635 *Environment*, 661, 449-464, <https://doi.org/10.1016/j.scitotenv.2019.01.146>, 2019.
- 636 Gleeson, T., Smith, L., Moosdorf, N., Hartmann, J., Dürr, H. H., Manning, A. H., van Beek, L. P. H., and Jellinek, A. M.  
637 (2011), Mapping permeability over the surface of the Earth, *Geophys. Res. Lett.*, 38, L02401,  
638 doi:10.1029/2010GL045565.
- 639 Guzzetti, F., Cardinali, M., Reichenbach, P. (1996). The influence of structural setting and lithology on landslide type and  
640 pattern. *Environmental and Engineering Geosciences*, 2, 531–555. doi:10.2113/gseegeosci.ii.4.531
- 641 Han, L., Fuqiang, L., Zheng, D., Weixu, X. (2018). A lithology identification method for continental shale oil reservoir based  
642 on BP neural network. *Journal of Geophysics and Engineering*, 15(3), 895–908. [https://doi.org/10.1088/1742-](https://doi.org/10.1088/1742-2140/aaa4db)  
643 [2140/aaa4db](https://doi.org/10.1088/1742-2140/aaa4db)
- 644 Hartmann, J., N. Jansen, H. H. Dürr, A. Harashima, K. Okubo, and S. Kempe (2010), Predicting riverine dissolved silica fluxes  
645 to coastal zones from a hyperactive region and analysis of their first order controls, *Int. J. Earth Sci.*, 99 (1), 207–230,  
646 doi:10.1007/s00531-008-0381-5
- 647 Hartmann, J., Dürr, H.H., Moosdorf, N., Meybeck, M., Kempe, S., 2012. The geochemical composition of the terrestrial  
648 surface (without soils) and comparison with the upper continental crust. *Int. J. Earth Sci.* 101, 365–376.  
649 <https://doi.org/10.1007/s00531-010-0635-x>
- 650 Hartmann, J., Moosdorf, N., 2012. The new global lithological map database GLiM: A representation of rock properties at the  
651 Earth surface: TECHNICAL BRIEF. *Geochem. Geophys. Geosystems* 13. <https://doi.org/10.1029/2012GC004370>
- 652 Horton, J.D., 2017, The State Geologic Map Compilation (SGMC) geodatabase of the conterminous United States (ver. 1.1,  
653 August 2017): U.S. Geological Survey data release, <https://doi.org/10.5066/F7WH2N65>.
- 654 Ispra & Parco Nazionale del Cilento, Vallo di Diano e Alburni (2013) - Carta geologica con elementi tematici e carta dei  
655 paesaggi sottomarini del Parco Nazionale del Cilento, Vallo di Diano e Alburni (European and Global Geopark).  
656 Salerno. [http://www.isprambiente.gov.it/it/progetti/suolo-eterritorio-1/carta-geologica-del-parco-del-cilento-vallo-di-](http://www.isprambiente.gov.it/it/progetti/suolo-eterritorio-1/carta-geologica-del-parco-del-cilento-vallo-di-diano-e-degli-alburni)  
657 [diano-e-degli-alburni](http://www.isprambiente.gov.it/it/progetti/suolo-eterritorio-1/carta-geologica-del-parco-del-cilento-vallo-di-diano-e-degli-alburni)
- 658 Lentini, F. & Carbone, S. Eds. (2014) - *Geologia della Sicilia. Mem. Descr. Carta Geol. d'It.*, 95: pp. 413, Serv. Geol. d'It.,  
659 Roma



- 660 Lombardo, L., Loche, M., Marchesini, I., Alvioli, M., Bakka, H. (2021). A strategy to obtain statistically significant landslide  
661 susceptibility maps from a spatially unbalanced, nation-wide inventory in Italy. Submitted for publication.
- 662 Lorenzo-Lacruz, J., Garcia, C., Morán-Tejeda, E., 2017. Groundwater level responses to precipitation variability in  
663 Mediterranean insular aquifers. *J. Hydrol.* 552, 516–531. <https://doi.org/10.1016/j.jhydrol.2017.07.011>
- 664 Marchesini, I., Cencetti, C., & De Rosa, P., 2009. A preliminary method for the evaluation of the landslides volume at a  
665 regional scale. *GeoInformatica*, 13(3), 277–289. <https://doi.org/10.1007/s10707-008-0060-5>
- 666 Marchesini, I., Mergili, M., Rossi, M., Santangelo, M., Cardinali, M., Ardizzone, F., Fiorucci, F., Schneider-Muntau, B., Fellin,  
667 W., & Guzzetti, F., 2014. A GIS Approach to Analysis of Deep-Seated Slope Stability in Complex Geology. In K.  
668 Sassa, P. Canuti, & Y. Yin (Eds.), *Landslide Science for a Safer Geoenvironment* (pp. 483–489). Springer International  
669 Publishing. [https://doi.org/10.1007/978-3-319-05050-8\\_75](https://doi.org/10.1007/978-3-319-05050-8_75)
- 670 Mergili, M., Marchesini, I., Rossi, M., Guzzetti, F., & Fellin, W., 2014a. Spatially distributed three-dimensional slope stability  
671 modelling in a raster GIS. *Geomorphology*, 206, 178–195. <https://doi.org/10.1016/j.geomorph.2013.10.008>
- 672 Mergili, M., Marchesini, I., Alvioli, M., Metz, M., Schneider-Muntau, B., Rossi, M., Guzzetti, F., 2014b. A strategy for GIS-  
673 based 3-D slope stability modelling over large areas. *Geosci. Model Dev.* 7, 2969–2982. <https://doi.org/10.5194/gmd-7-2969-2014>
- 674
- 675 Ministero dei Lavori Pubblici, Ufficio Idrografico, Sezione Geologica (1948) - Carta Geologica d'Italia alla scala 1:100.000 –  
676 F. 35 Riva. Firenze.
- 677 Mirabella, F., Bucci, F., Santangelo, M., Cardinali, M., Caielli, G., De Franco, R., Guzzetti, F., & Barchi, M. R. (2018).  
678 Alluvial fan shifts and stream captures driven by extensional tectonics in central Italy. *Journal of the Geological Society*,  
679 175, 788–805. <https://doi.org/10.1144/jgs2017-138>.
- 680 Mori, F., Mendicelli, A., Moscatelli, M., Romagnoli, G., Peronace, E., Naso, G., 2020. A new Vs30 map for Italy based on the  
681 seismic microzonation dataset. *Eng. Geol.* 275, 105745. <https://doi.org/10.1016/j.enggeo.2020.105745>
- 682 Novellino, R., Bucci, F., Tavarnelli, E., 2021. Structural investigation of background features and normal faults affecting the  
683 Calcari con Selce Formation, Southern Apennines, Italy. *Ital. J. Geosci.* 140, 1–21. <https://doi.org/10.3301/ijg.2020.31>
- 684 Onegeology: <http://www.onegeology.org/portal/home.html> (access date 2021/05/07)
- 685 Pantaloni, M. (2011) - La Carta geologica d'Italia alla scala 1:1.000.000: una pietra miliare nel percorso della conoscenza  
686 geologica. *Geologia Tecnica & Ambientale*, 2-3(11): 88-99
- 687 Patacca, E., Scandone, P., Bellatalla, M., Perilli, N., Santini, U. (1991) - La zona di giunzione tra l'arco Appennino  
688 settentrionale e l'arco Appennino meridionale nell'Abruzzo e nel Molise. *Studi Geol. Camerti*, Vol. Spec. 2: 417-441.
- 689 Piana, F., Fioraso, G., Irace, A., Mosca, P., d'Atri, A., Barale, L., Falletti, P., Monegato, G., Morelli, M., Tallone, S., Vigna,  
690 G.B., 2017. Geology of Piemonte region (NW Italy, Alps–Apennines interference zone). *J. Maps* 13, 395–405.  
691 <https://doi.org/10.1080/17445647.2017.1316218>



- 692 Prosser, G. (2000) The development of the North Giudicarie fault zone (Insubric line, Northern Italy). *Journal of Geodynamics*,  
693 30, 1-2, 229-250
- 694 R. Ufficio Geologico (1884a) - Carta Geologica d'Italia alla scala 1:100.000 – F. 248 Trapani. Roma.
- 695 R. Ufficio Geologico (1884b) - Carta Geologica d'Italia alla scala 1:100.000 – F. 249 Palermo. Roma.
- 696 R. Ufficio Geologico (1884c) - Carta Geologica d'Italia alla scala 1:100.000 – F. 257 Castevetrano. Roma.
- 697 R. Ufficio Geologico (1884d) - Carta Geologica d'Italia alla scala 1:100.000 – F. 258 Corleone. Roma.
- 698 R. Ufficio Geologico (1884e) - Carta Geologica d'Italia alla scala 1:100.000 – F. 266 Sciacca. Roma.
- 699 R. Ufficio Geologico (1900) - Carta Geologica d'Italia alla scala 1:100.000 – F. 228 Cetraro. Roma.
- 700 Raia, S., Alvioli, M., Rossi, M., Baum, R.L., Godt, J.W., Guzzetti, F., 2014. Improving predictive power of physically based  
701 rainfall-induced shallow landslide models: a probabilistic approach. *Geosci. Model Dev.* 7, 495–514.  
702 <https://doi.org/10.5194/gmd-7-495-2014>
- 703 Reichenbach, P., Rossi, M., Malamud, B.D., Mihir, M., Guzzetti, F., 2018. A review of statistically-based landslide  
704 susceptibility models. *Earth-Sci. Rev.* 180, 60–91. <https://doi.org/10.1016/j.earscirev.2018.03.001>
- 705 Roche, V., Bouchot, V., Beccalotto, L., Jolivet, L., Guillou-Frottier, L., Tuduri, J., Bozkurt, E., Oguz, K., Tokay, B., 2019.  
706 Structural, lithological, and geodynamic controls on geothermal activity in the Menderes geothermal Province (Western  
707 Anatolia, Turkey). *Int. J. Earth Sci.* 108, 301–328. <https://doi.org/10.1007/s00531-018-1655-1>
- 708 Ronchi, A., Cassinis, G., Durand, M., Fontana, D., Oggiano, G., Stefani, C., 2011. Stratigrafia e analisi di facies della  
709 successione continentale permiana e triassica della Nurra: confronti con la Provenza e ricostruzione paleogeografica.  
710 *Geol. Field Trips* 3, 1–43. <https://doi.org/10.3301/GFT.2011.01>
- 711 Rossi, M., Reichenbach, P., 2016. LAND-SE: a software for statistically based landslide susceptibility zonation, version 1.0.  
712 *Geosci. Model Dev.* 9, 3533–3543. <https://doi.org/10.5194/gmd-9-3533-2016>
- 713 Sarro, R., Mateos, R. M., Reichenbach, P., Aguilera, H., Riquelme, A., Hernández-Gutiérrez, L. E., Martín, A., Barra, A.,  
714 Solari, L., Monserrat, O., Alvioli, M., Fernández-Merodo, J. A., López-Vinielles, J., Herrera, G. (2021). Geotechnics  
715 for rockfall assessment in the volcanic island of Gran Canaria (Canary Islands, Spain). *Journal of Maps* 16(2), 605-613  
716 (2020).
- 717 Santangelo, M., Gioia, D., Cardinali, M., Guzzetti, F., & Schiattarella, M. (2013). Interplay between mass movement and  
718 fluvial network organization: An example from southern Apennines. *Italy Geomorphology*, 188, 54–67.
- 719 Schiattarella, M., Beneduce, P., Di Leo P., Giano, S.I., Giannandrea, P., Principe, C. (2005) - Assetto strutturale ed evoluzione  
720 morfotettonica quaternaria del vulcano del Monte Vulture (Appennino lucano). *Boll. Soc. Geol. It.*, 124: 543-562.
- 721 Schlögel, R., Marchesini, I., Alvioli, M., Reichenbach, P., Rossi, M., Malet, J.-P., 2018. Optimizing landslide susceptibility  
722 zonation: Effects of DEM spatial resolution and slope unit delineation on logistic regression models. *Geomorphology*  
723 301, 10–20. <https://doi.org/10.1016/j.geomorph.2017.10.018>



- 724 Servizio Geologico d'Italia (1955) - Carta Geologica d'Italia alla scala 1:100.000 – F. 265 Mazzara del Vallo. Firenze.
- 725 Servizio Geologico d'Italia (1964) - Carta Geologica d'Italia alla scala 1:100.000 – F. 163 Lucera. E.I.R.A., Firenze.
- 726 Servizio Geologico d'Italia (1965) - Carta Geologica d'Italia alla scala 1:100.000 – F. 185 Salerno. E.I.R.A., Firenze
- 727 Servizio Geologico d'Italia (1968a) - Carta Geologica d'Italia alla scala 1:100.000. F. 122 Perugia. Bergamo.
- 728 Servizio Geologico d'Italia (1968b) - Carta Geologica d'Italia alla scala 1:100.000 – F. 36 Schio. Bergamo.
- 729 Servizio Geologico d'Italia (1969) - Carta Geologica d'Italia alla scala 1:100.000 – F. 199 Potenza. Roma.
- 730 Servizio Geologico d'Italia (1970a) - Carta Geologica d'Italia alla scala 1:100.000 – F. 34 Breno. E.I.R.A., Firenze
- 731 Servizio Geologico d'Italia (1970b) - Carta Geologica d'Italia alla scala 1:100.000 – F. 186 S. Angelo dei Lombardi. Ercolano
- 732 (Napoli)
- 733 Servizio Geologico d'Italia (1970c) - Carta Geologica d'Italia alla scala 1:100.000 – F. 220 Verbicaro. Ercolano (Napoli)
- 734 Servizio Geologico d'Italia (1970d) - Carta Geologica d'Italia alla scala 1:100.000 - F. 198 Eboli. Roma.
- 735 Servizio Geologico d'Italia (1970e) - Carta Geologica d'Italia alla scala 1:100.000 – F. 187 Melfi. Ercolano (Napoli).
- 736 Servizio Geologico d'Italia (1972) - Carta Geologica d'Italia alla scala 1:50.000, F. 027 Bolzano, Firenze.
- 737 Servizio Geologico d'Italia (1977) - Carta Geologica d'Italia alla scala 1:50.000, F. 028 La Marmolada, Firenze.
- 738 Servizio Geologico d'Italia (2002) - Carta Geologica d'Italia in scala 1:50.00, F. 132-152-153, Bardonecchia.
- 739 Servizio Geologico d'Italia (2004) - Carta geologica d'Italia interattiva. Interactive geological map of Italy: 1:100.000. 3 CD.
- 740 M. AMANTI, R. BONTEMPO, P. CARA (a cura di). 1a edizione, Realizzato da Etruria innovazione.
- 741 Servizio Geologico d'Italia (2005a) - Carta Geologica d'Italia alla scala 1:50.000, F. 503 Vallo della Lucania. APAT, Roma.
- 742 Servizio Geologico d'Italia (2005b) - Carta geologica d'Italia alla scala 1:50.000, F. 256 Rimini. APAT, Roma.
- 743 Servizio Geologico d'Italia (2005c) - Carta Geologica d'Italia alla scala 1:1.250.000. APAT, S.EL.CA., Firenze.
- 744 Servizio Geologico d'Italia (2005d) - Carta Geologica d'Italia alla scala 1:50.000, F. 215 Bedonia. APAT, Roma.
- 745 Servizio Geologico d'Italia (2006) - Carta Geologica d'Italia alla scala 1:50.000, F. 214 Bargagli. APAT, Roma.
- 746 Servizio Geologico d'Italia (2008) - Carta Geologica d'Italia alla scala 1:50.000, F. 058 Monte Adamello. APAT, Roma.
- 747 Servizio Geologico d'Italia (2009a) - Carta Geologica d'Italia alla scala 1:50.000, F. 031 Ampezzo. ISPRA, Roma.
- 748 Servizio Geologico d'Italia (2009b) - Carta Geologica d'Italia alla scala 1:50.000, F. 599 Patti. ISPRA, Roma.
- 749 Servizio Geologico d'Italia (2010a) - Carta Geologica d'Italia alla scala 1:50.000, F. 258-271 San Remo. ISPRA, Roma.
- 750 Servizio Geologico d'Italia (2010b) - Carta Geologica d'Italia alla scala 1: 50.000, F. 504 Sala Consilina. ISPRA, Roma.
- 751 Servizio Geologico d'Italia (2010c) - Carta Geologica d'Italia alla scala 1:50.000, F. 228 Cairo Montenotte. ISPRA, Roma.
- 752 Servizio Geologico d'Italia (2011a) - Carta Geologica d'Italia alla scala 1:50.000, F. 99 Iseo. ISPRA, Roma.
- 753 Servizio Geologico d'Italia (2011b) - Carta Geologica d'Italia alla scala 1:50.000, F. 089 Courmayeur. ISPRA, Roma.
- 754 Servizio Geologico d'Italia (2011c) - Carta Geologica d'Italia alla scala 1:50.000, F. 587-600 Milazzo-Barcellona P. di G.,
- 755 S.EL.CA., Firenze.



- 756 Servizio Geologico d'Italia (2011d) - Carta Geologica d'Italia alla scala 1:1.000.000. ISPRA, Roma.
- 757 Servizio Geologico d'Italia (2012a) - Carta Geologica d'Italia alla scala 1:50.000, F. 564 Carbonia. ISPRA, Roma.
- 758 Servizio Geologico d'Italia (2012b) - Carta Geologica d'Italia alla scala 1:50.000, F. 098 Bergamo. ISPRA, Roma.
- 759 Servizio Geologico d'Italia (2012c) - Carta Geologica d'Italia alla scala 1: 50.000, F. 489 Marsico Nuovo. ISPRA, Roma.
- 760 Servizio Geologico d'Italia (2014) - Carta Geologica d'Italia alla scala 1: 50.000, F. 505 Moliterno. ISPRA, Roma.
- 761 Servizio Geologico d'Italia (2015a) - Carta Geologica d'Italia alla scala 1:50.000, F. 555 Iglesias. ISPRA, Roma.
- 762 Servizio Geologico d'Italia (2015b) - Carta Geologica d'Italia alla scala 1: 50.000, F. 580 Soverato. ISPRA, Roma.
- 763 Servizio Geologico d'Italia (2015c) - Carta Geologica d'Italia alla scala 1:50.000, F. 070 Monte Cervino. ISPRA, Roma.
- 764 Servizio Geologico d'Italia (2016) - Carta Geologica d'Italia alla scala 1:50.000, F. 280 Fossombrone. ISPRA,
- 765 Roma.
- 766 Tavarnelli E. (1997) - Structural evolution of a foreland fold-and-thrust belt: the Umbria-Marche Apennines, Italy. *Journal of*
- 767 *Structural Geology*, 19, 523-534
- 768 Trigila, A., Iadanza, C., & Spizzichino, D. (2010). Quality assessment of the Italian landslide inventory using GIS processing.
- 769 *Landslides*, 7(4), 455–470. <https://doi.org/10.1007/s10346-010-0213-0>
- 770 UNESCO-IUGS (2016) – International Stratigraphic chart (versione aggiornata reperibile nel sito:
- 771 <http://www.stratigraphy.org/index.php/ics-chart-timescale>)
- 772 Vanmaercke, M., Panagos, P., Vanwalleghem, T., Hayas, A., Foerster, S., Borrelli, P., Rossi, M., Torri, D., Casali, J., Borselli,
- 773 L., Vigiak, O., Maerker, M., Haregeweyn, N., De Geeter, S., Zgłobicki, W., Biielders, C., Cerdà, A., Conoscenti, C., de
- 774 Figueiredo, T., Evans, B., Golosov, V., Ionita, I., Karydas, C., Kertész, A., Krása, J., Le Bouteiller, C., Radoane, M.,
- 775 Ristić, R., Rousseva, S., Stankoviansky, M., Stolte, J., Stolz, C., Bartley, R., Wilkinson, S., Jarihani, B., Poesen, J.,
- 776 2021. Measuring, modelling and managing gully erosion at large scales: A state of the art. *Earth-Sci. Rev.* 103637.
- 777 <https://doi.org/10.1016/j.earscirev.2021.103637>
- 778 Vezzani, L., Festa, A., Ghisetti, F.C., 2010. Geology and tectonic evolution of the central-southern Apennines, Italy, Special
- 779 paper. Geological Society of America, Boulder, Colo.
- 780 Vignaroli, G., Mancini, M., Bucci, F., Cardinali, M., Cavinato, G. P., Moscatelli, M., Putignano, M. L., Sirianni, P., Santangelo,
- 781 M., Ardizzone, F., Cosentino, G., Di Salvo, C., Fiorucci, F., Gaudiosi, I., Giallini, S., Messina, P., Peronace, E.,
- 782 Polpetta, F., Reichenbach, P.,...Stigliano, F. (2019). Geology of the central part of the Amatrice Basin (Central
- 783 Apennines, Italy). *Journal of Maps*, 15(2), 193–202. <https://doi: 10.1080/17445647.2019.1570877>.
- 784 Vojtek, M., Vojteková, J. 2019.: Flood Susceptibility Mapping on a National Scale in Slovakia Using the Analytical Hierarchy
- 785 Process. *Water* 2019, 11, 364. <https://doi.org/10.3390/w11020364>
- 786
- 787
- 788



789

## APPENDIX

790

### Data acquisition procedure

791 ISPRA exhibits a REST service for the publication of spatial data (Table 1, ID 9). The acronym REST stands for  
792 "REpresentational State Transfer", which is an architectural style to develop services using the http data transfer protocol. In  
793 particular, ISPRA uses the ArcGIS REST API, the Advanced Programming Interface REST developed by ESRI through the  
794 proprietary ArcGIS Online platform. The ESRI API can be queried through specific http requests (for example of GET type,  
795 in which the service address is followed by a series of key-value information) that allow, for example, to obtain the  
796 representation in JSON (JavaScript Object Notation) format of geometries (geospatial layer features) and associated attributes.  
797 Normally this service is limited to the return of a maximum number of features for each request. The acquisition of the database  
798 required (i) knowledge of the REST service APIs and (ii) a procedure for the automatic download of subsets of data, which  
799 cannot be downloaded in a single piece by design of the website, and (iii) merging of all of the subsets into a single vector  
800 map. To execute the download, we prepared a script to download subsets of 100 polygons (geometric features) for each single  
801 call to the service, using the Linux *wget* command. The procedure is simple, and consists of a loop in which, at each iteration,  
802 a number ( $\Delta$ ) of polygons (100, in the actual case), out of the 300,000 total available polygons. Given that the API of the REST  
803 service database was unknown to us, we followed a trial-and error procedure to obtain a working script. Downloaded data  
804 consisted of 2,927 files in GeoJSON format, which we converted to a single ESRI Shapefile using the GDAL/OGR library.

805